Winter 2019

Modeling the Effects of Climate Variability on Hydrology and Stream Temperatures in the North Fork of the Stillaguamish River

Kyra Freeman
Western Washington University, kyrafreeman4@gmail.com

Modeling the Effects of Climate Variability on Hydrology and Stream Temperatures in the North Fork of the Stillaguamish River

By

Kyra Freeman

Accepted in Partial Completion of the
Requirements for the Degree
Master of Science

ADVISORY COMMITTEE

Dr. Robert Mitchell, Chair

Dr. Doug Clark

Dr. John Yearsley

GRADUATE SCHOOL

Dr. Gautam Pillay, Dean

Master's Thesis

In presenting this thesis in partial fulfillment of the requirements for a master's degree at Western Washington University, I grant to Western Washington University the non-exclusive royalty-free right to archive, reproduce, distribute, and display the thesis in any and all forms, including electronic format, via any digital library mechanisms maintained by WWU.

I represent and warrant this is my original work, and does not infringe or violate any rights of others. I warrant that I have obtained written permissions from the owner of any third party copyrighted material included in these files.

I acknowledge that I retain ownership rights to the copyright of this work, including but not limited to the right to use all or part of this work in future works, such as articles or books.

Library users are granted permission for individual, research and non-commercial reproduction of this work for educational purposes only. Any further digital posting of this document requires specific permission from the author.

Any copying or publication of this thesis for commercial purposes, or for financial gain, is not allowed without my written permission.

Kyra Freeman

March 1, 2019

Modeling the Effects of Climate Variability on Hydrology and Stream Temperatures in the North Fork of the Stillaguamish River

A Thesis
Presented to
The Faculty of
Western Washington University

In Partial Fulfillment
Of the Requirements for the Degree
Master of Science

by
Kyra Freeman
March 2019

Abstract

The Stillaguamish River in northwest Washington State, USA, provides water resources to local agriculture, industry and First Nations Tribes, and provides crucial habitat for several endangered species of salmonids. The watershed experiences a mild maritime climate and high relief, with rain and snowmelt dominating the streamflow. In anticipation of shifts in snowpack, streamflow, and stream temperature, I use projected global climate scenarios and numerical models to examine future climatic variability on streamflow and stream temperatures in the snow-melt dominated North Fork of the Stillaguamish River. I calibrated the physically based Distributed Hydrology Soil Vegetation Model (DHSVM) and River Basin Model (RBM) to gridded historical meteorological data in the basin and then applied downscaled, gridded projected climate data to predict streamflow and stream temperature changes through 2090 in this basin.

Forecast modeling indicates that the North Fork watershed will transition from a snow- to rain-dominated basin into the 21st century as a result of increasing air temperatures. More precipitation in the winter will fall as rain rather than snow, resulting in up to a 43% increase in streamflow and a 56% decline in basin-wide snowpack. The reduced snowpack will melt out earlier and cause a decrease in spring and summer streamflow. Simulations of stream temperature indicate rising temperatures in every stream segment in the basin by the end of the 21st century as a result of higher air temperatures, declining snowpack, and lower summer streamflow. Monthly average stream temperatures could increase by up to 7.4 ^{o}C. In addition, the temperature thresholds for every life cycle of endangered salmon species are increasingly exceeded through time, putting at risk already endangered salmon species. By the end of the 21st century, the main stem may experience up to a 10-fold increase in number of days per year exceeding salmon temperature thresholds. Reach-scale predictions of stream temperature trends through the basin offer water resource managers a tool for focusing riparian and groundwater restoration efforts.

Acknowledgements

This project was funded by the Stillaguamish Tribe, the Northwest Climate Science Adaptation Center, the Geology Department of Western Washington University, and the Western Washington University Office of Research and Sponsored Programs.

I am grateful to Bob Mitchell, my thesis supervisor, for his support and guidance during the last two years. I could have not completed this project in a timely manner without the continued attention, time, and advise that he provided every step of the way. Thank you for your commitment to this project. Thank you to John Yearsley for spending some of his valuable retirement time teaching me about the River Basin Model. Thanks to Doug Clark for and for valuable feedback and thoughts throughout this project. Thank you to all employees of the Stillaguamish Tribe that have supported this project, particularly to Kip Killebrew who spent a lot time developing improved methods to install temperature sensors. My field work would not have been successful without him. Thanks to Molly Johnson, Tristan Coragiulo, and Kate Clarke for additional field work assistance. Thank you to those involved in producing the various public datasets that made this study possible. I am grateful to Jim Long who provided invaluable IT support and scripts that streamlined the forecasted modeling. Throughout this project, I relied on methods tested in the Nooksack River basin by Ryan Murphy and Stephanie Truitt. I appreciate the time they both took to answer questions and make their research available to me. Finally, thank you to Mike Coons for IT support, field work support, and being an understanding distraction throughout this project.

Table of Contents

List of Tables

List of Figures

1.0 Introduction

The Stillaguamish River in Washington State, USA, provides water resources to regional agriculture, industry and First Nations Tribes, and is an important salmon habitat (Figure 1). The Stillaguamish Tribe relies on the Stillaguamish River for both traditional and economic salmon fishing and for promoting cultural environmental stewardship practices. In anticipation of shifts in snowpack, streamflow, and stream temperature as a result of forecasted climate change, there is a rising demand from local and regional stakeholders for stream hydrology and stream temperature projections to predict the timing of detrimental conditions for aquatic ecosystems.

Because of the mild maritime climate of the Pacific Northwest (PNW), the Stillaguamish River basin experiences winter precipitation as both rain and snow. In Washington State, rain-snow transitional basins such as the Stillaguamish are projected to be most sensitive to climate warming as subtle temperature fluctuations dictate whether precipitation falls as rain or snow (Elsner et al., 2010; Mantua et al., 2010). Orographic effects caused by the steep relief of the Stillaguamish basin can produce precipitation magnitudes in excess of 350 cm/year (PRISM Climate Group, 2014). The basin receives approximately 75% its precipitation between October and March (SIRC, 2005). Precipitation falls primarily as rain in the fall months, producing rapid runoff to streams when snowpack is limited. Snow accumulation develops in the winter when temperatures decrease, and historically reaches a peak around April 1. About 46% of the basin is 300-900 m elevation and could experience rain or snow in the winter months (SIRC, 2005). Spring and early summer streamflow in the Stillaguamish is currently supported by snowmelt,

which, in part, buffers summer stream temperatures. Stream temperature is influenced by a variety of factors, including air temperature, solar and longwave radiation, streamflow, channel width, and riparian cover.

My study focused on predicting hydrology and stream temperature changes in the North Fork tributary due to climate warming into the 21st century. The North Fork contributes about half of the total discharge in the Stillaguamish River, the fifth largest river draining to the Puget Sound. The North Fork drains an area of 734 km^2 with relief ranging from 55 m to 2100 m. The annual mean discharge recorded at a USGS stream gauge near the mouth of the North Fork is about 57 cms with peak flows on the order of 280 -1,400 cms, typically in the fall and winter (Figure 1—2; USGS, 2017). Low flows of about 11 cms occur in the dry season between July and October (USGS, 2017). The Washington Department of Ecology (WADOE) installed a streamflow and stream temperature monitoring station in the main stem of the North Fork of the Stillaguamish in 2004, upstream of the USGS gauge (Figures 1—2). Between 2004-2012, the average daily temperature was 8.6 ^oC. The minimum average daily temperature occurred on December 20, 2008 at 0.2 ^oC and the maximum average daily temperature occurred on July 28 and 29, 2009, both at 19.2 ^oC.

Increasing levels of carbon dioxide and other greenhouse gases in the Earth's atmosphere have and will continue to increase average global air temperatures through the greenhouse effect (Diffenbaugh et al., 2017). Global and regional weather patterns will also continue to change as a result of changes to Earth's energy budget. In a 2014 report, the U.S. Global Change Research Program predicted the average annual air temperature to increase by 3.4 ^oC in the PNW by 2099 (Mote et al., 2014). To date, annual mean air temperatures in the PNW have increased by 0.6 -

0.8 ^{o}C from 1901 to 2012 (Abatzoglou et al., 2013). Projected trends are expected to show an increase in frequency and intensity of winter precipitation events in western Washington (Mauger et al., 2016), though annual precipitation shows variable trends that seem to relate more to year-to-year variations in climate than any long term trends (Abatzoglou et al., 2013). The University of Washington Climate Change Impact Group (UW-CIG) estimates that the early spring snow pack will decrease by 59% by the 2080s, and that as a consequence, seasonal streamflow peaks will likely shift significantly in their timing and magnitude (Littell et al., 2009). Projected increases in air temperature will not only negatively influence the magnitudes of melt water and amount of flow but will also directly increase stream temperatures.

Forecasted climate data used in this study were generated from different Global Climate Models (GCMs) developed by various organizations such as NASA Goddard Institute for Space Studies, the Meteorological Research Institute, and the Institute Pierre Simon Laplace (Rupp et al., 2013). GCMs produce numerical estimations of the climate-driven thermodynamic changes that are likely to occur based on different simulations of Earth's ocean and atmospheric circulation. Historic gridded climate data developed by Livneh et al. (2013) was used for hydrologic and stream temperature model calibration.

Previous modeling investigations in the region have used the Distributed Hydrology Soil Vegetation Model (DHSVM) to predict streamflow (e.g., Dickerson-Lange and Mitchell, 2014; Murphy 2016; Cao et al., 2016) and the River Basin Model (RBM) to predict stream temperature (e.g., Sun et al. 2014; Cao et al., 2016; Truitt, 2018). To the north of the Stillaguamish, the South Fork of the Nooksack River is physically and geographically similar to the North Fork Stillaguamish. Employing DHSVM, Dickerson-Lange and Mitchell (2014) and Murphy (2016)

predicted an increase in winter flow, a decrease in summer flow, and an earlier and lower spring peak streamflow corresponding with a decrease in basin-wide snowpack. In particular, Murphy (2016) found that DHSVM simulations predicted that winter median streamflow will more than double by 2075 as a result of increased precipitation falling as rain in place of snow. Truitt (2018) modeled stream temperature in three Nooksack basins with RBM and found that the highest simulated stream temperatures near the end of the 21st century occur in the unglaciated South Fork Nooksack basin, the basin most comparable to the North Fork Stillaguamish.

Cao et al. (2016) used the DHSVM and RBM to examine streamflow and temperature of fifteen major streams discharging to the Puget Sound at a 150 m gridded resolution. Based on forecasted climate data, Cao et al. concluded that the Stillaguamish basin will have an average of over 50 days per year where the maximum daily temperature recorded at the river outlet that will exceed 20 ^{o}C by the mid-21st century, the highest of any river draining into the Puget Sound. While different salmon species will have varying responses to stream temperature based on their life cycle stage (Beechie et al, 2013; Mantua et al., 2010), the optimal range for adult Chinook salmon migration is between 3.3 and 13.3 ^{o}C (Black et al., 2003), and the lethal threshold for adult Chinook is consistent temperatures around 22 ^{o}C (WADOE, 2008). The 50 days approaching this threshold are predicted to occur in the warmest months (August/September) which correspond to the timing of the Chinook summer runs. Cao et al. also found that summer stream temperatures could be buffered by riparian shading, but acknowledged that the riparian input parameters used for their model were assumed to be uniform throughout the study area with tree heights of 10 m, buffer width of 5 m, a Leaf Area Index (LAI) of 5, and a bank to canopy height of 0.01 m. Although Cao et al. used uniform riparian values, they likely vary

considerably along the stream channels. Air temperatures differences between open and below canopy locations typically vary by 5 ^{o}C (Leach et al., 2016), and fluctuations in canopy cover will directly impact the stream temperature.

Forecasted streamflow and stream temperature trends are expected to inform salmon habitat restoration decisions made by the Stillaguamish Tribe and other water resource interests. The Stillaguamish basin contains critical habitat for eight salmonid species, three of which have been listed as threatened by the Endangered Species Act since 1999. In particular, the endangered Chinook salmon species are of high cultural and economic importance to the Stillaguamish Tribe, and it is estimated that salmon populations returning to the Stillaguamish River decreased 90% through the 20th century (SIRC, 2005). The summer-run Chinook mainly use the North Fork Stillaguamish tributary, enter the river after late May and spawn in late August-late October (PSIT & WDFW, 2017). Summer stream temperature increases can cause salmon species to be more at risk to disease, and is linked to loss of salmon migration capabilities, and lowers the dissolved oxygen content of the water endangering developing salmon embryos (Wade et al., 2013; Cao et al., 2016). A 2005 report outlining salmon recovery recommendations includes a list of habitat goals for the Stillaguamish River, and states that stream temperature should ideally not exceed 12-14 ^{o}C (SIRC, 2005).

An extensive Total Maximum Daily Load (TMDL) water quality study of the Stillaguamish basin was conducted by Snohomish County, with investigations of factors such as groundwater seepage, stream temperature, flow analyses, and riparian conditions (SCSWM, 2015). Recommendations to improve stream temperature for aquatic health in the watershed include constructing engineer log jams that scour deep pools and provide cold-water refuge for aquatic

species, planting riparian corridors along key river segments, and restoring vegetation that has been de-forested (Leonetti et al., 2015). In the Stillaguamish basin, land use is estimated as 76% forestry, 17% rural, 5% agriculture, and 2% urban. Of the forested land, about half is federally owned and managed for timber production. In the North Fork, this translates to 45 km^2 of forestry land. While still a productive industry, logging activity has decreased since the early 1990s as a response to changing markets and the implementation of environmental laws (SIRC, 2005).

I applied historical and forecasted climate data to force the DHSVM and RBM in the North Fork Stillaguamish basin in order to examine streamflow and stream temperature trends over the 21st century. Both models are physically based and distributed and have been applied in mountainous terrain in the PNW (e.g., Vano et al., 2010; Cuo et al., 2011; Dickerson-Lange and Mitchell, 2014; Murphy, 2016; Cao et al., 2016; Truitt, 2018). To account for the effects of landscape heterogeneity on hydrologic systems, I modeled hydrology at a higher (50 m) spatial resolution, and to account for stream temperature fluxes because of vegetation variability, I used more detailed riparian inputs than Cao et al. (2016). To predict which reaches could most benefit from vegetation restoration and improved riparian conditions, I compared stream temperature forecast results generated with present-day riparian and vegetation conditions with stream temperature forecasts based on pre-industry forest conditions using the 1883 land cover and riparian conditions of Cao et al. (2016). Pre-industrial vegetation conditions represent the upper bounds of the remediation potential of the basin and was used as a demonstrative tool. My results identify reaches that are most at risk of temperature increases and highlight areas where habitat rehabilitation funds could be allocated.

2.0 Methods

I applied the DHSVM and RBM models to assess changing hydrology and stream temperatures in the North Fork of the Stillaguamish River basin resulting from projected climate change with the goal of identifying stream reaches at risk of becoming less hospitable to salmon. I accomplished this objective with the following scope of work.

1. Created a 50 m gridded digital basin using inputs from government agencies and ArcGIS software.
2. Constructed a riparian buffer along all stream reaches using lidar data to quantify vegetation height. Created vegetation file to inform riparian conditions along each individual stream reach.
3. Calibrated and validated the DHSVM using the gridded historical meteorological data and historic USGS gauge streamflow data.
4. Conducted field work to measure stream discharge, temperature, and morphology, used to determine the Mohseni and Leopold parameters required as inputs for the RBM.
5. Calibrated and validated RBM using gridded historical meteorological data and historic WADOE historic temperature data and calculated Mohseni and Leopold parameters from field work.
6. Performed DHSVM and RBM simulations using gridded downscaled forecasted meteorological data to determine projected stream temperature. Performed simulations a second time with 1883 vegetation conditions.

7. Processed and statistically analyzed data using the software R. Determined stream sub-basins that are particularly at-risk for temperature increases and significant streamflow changes.

2.1 Digital Spatial Characterization

Both the DHSVM and RBM are spatially distributed and require digital basin attributes. Detailed procedures for processing the digital inputs using ArcGIS are outlined in previous MS theses (e.g., Dickerson, 2010; Murphy, 2016). For the North Fork, light detection and ranging (lidar) data available from the Washington State Department of Natural Resources at 0.9 and 1.8 m resolutions were merged and resampled to a 50 m resolution. Land cover at a 30 m resolution from the National Oceanic and Atmospheric Association (NOAA) was resampled to 50 m and converted to DHSVM classes; soil types were acquired from the United States Department of Agriculture STATGO data base; and a soil thickness layer and stream network was generated using a Python-ArcGIS script developed for the DHSVM (Ning Sun, personal communication, 2017). A 150 m land cover layer from Cao et al. (2016) was resampled to a 50 m grid and used as an estimation of an 1883 land cover. The stream network contains 1730 individual stream segments.

2.2 Riparian Conditions

Riparian vegetation parameters for each of the 1730 stream segments are required as input for the DHSVM which produces energy outputs required for the RBM. Parameters include vegetation height along the stream, buffer width, or the width of the vegetation that provides shade to the stream, monthly extinction coefficient, a measure expressing the structure of the

canopy and the amount of light that is able to penetrate it, bank-to-canopy distance, or how close to the vegetation is to the stream edge, stream width, and overhang coefficient, which is the ratio of the stream width that is effected by shading (Table 1). Riparian buffer zone conditions were determined by a combination of lidar data, land cover data from NOAA, and Cao et al. (2016). Lidar data are collected by airborne laser scanners that analyze landscapes below using reflection calculations to determine the canopy height of vegetation and the structure of the terrain ("bare earth") below that (Kim et al., 2009). A Digital Surface Model (DSM) is generated by the "first return" reflections from the plane and models the tops of trees and other vegetation. A Digital Terrain Model (DTM) is generated by the beams that can penetrate the vegetation and reflect back to the plane ("last returns"). The DSM and DTM lidar data exist for the majority of the North Fork Basin at a 0.9 to 1.8 m resolution, respectively. The height of the vegetation at a 1.8 m resolution is determined by subtracting DTM data from DSM data.

A 10 m-wide riparian buffer around each stream segment in the network was generated, and this buffer was used to extract the lidar tree height in this area using a geoprocessing tool that I developed in ArcGIS Model Builder (Appendix A). A Python script was used to estimate the average height of vegetation within the buffer at each stream segment (Appendix A). Based on Sun et al. (2014), the extinction coefficient (k) was estimated as:

$$\boldsymbol{k = \frac{LAI}{64}} \qquad (1)$$

LAI was determined at each individual stream segment based on the DHSVM land cover vegetation type that was most dominant at each stream segment. Channel width was estimated to be 5 m in the tributaries, and 10 m along the main stem of the North Fork. A basin-wide average

of the overhang coefficient and the bank-to-canopy distance was used based on 2002 values used in Cao et al. (2016) (Table 1). The 1883 riparian conditions were estimated using basin-wide averages following Cao et al. (2016) values for a thick forest of mostly old-growth Douglas Fir trees in the upper reaches and mixed forest along the main stem. Tree height was input as 62 m, buffer width as 50 m, and LAI as 9. These values are consistent with quantitative measurements of Douglas Fir forests (Parker et al., 2002).

2.3 DHSVM Hydrology Calibration

The DHSVM was developed by Wigmosta et al. (1994) at the University of Washington and the Pacific Northwest National Lab and has been used extensively in mountainous terrain in the PNW (e.g., Vano et al., 2010; Cuo et al., 2011; Dickerson-Lange and Mitchell, 2014; Murphy, 2016). I used DHSVM 3.1.2 which was modified to produce the energy and streamflow inputs required for the RBM (PNNL, 2018). The spatially distributed model performs an energy and water balance on a gridded basin defined by a digital topography model, soil type, soil depth, vegetation cover, and stream network. The DHSVM uses physical relationships based on the gridded spatial inputs and meteorological data to simulate hydrology variables such as snow accumulation and melt, evapotranspiration, soil storage, and overall streamflow. The high level of spatial resolution allows for variability in topography, soil and land cover, and meteorology, resulting in a more accurate representation of the hydrology of a basin.

I used gridded historical meteorological datasets developed by Livneh et al. (2013) for the calibration. The resolution of the historical data is $1/16^{th}$ of a degree latitude/longitude and contains daily time series of climate variables at gridded points (hereafter referred to as “Livneh

nodes") from 1950-2013. The daily Livneh node data (minimum and maximum temperature, precipitation, and wind speed) were bias corrected, processed into variables required for the DHSVM, and disaggregated into 3-hr times steps by the UW-CIG (Mauger et al., 2016). Required DHSVM meteorological variables include air temperature (^{o}C), wind speed (m/s), humidity (%), solar radiation (W/m^2), longwave radiation (W/m^2), and precipitation (m). The data were validated against measured observations from the Finney Creek, Gold Hill, and Arlington weather stations that encompass the North Fork basin.

Calibration of DHSVM was achieved by forcing the model with the gridded historic meteorological data and adjusting model parameters one parameter at a time based on comparisons to observed streamflow data from USGS gauging station (12167000) located along the lower main stem of the North Fork Stillaguamish near Arlington, WA (Figure 1). Following the cross-validation method described in Bennett et al. (2013), the streamflow data were split into two groups. I used a ten-year period from 2003-2012 for model development and calibration. The second group of data, from 1983-2002 was used to verify the model and validate calibration results. The gauge was moved to its present location in 1989 and was in a downstream location from 1928-1989. The average discharge of the ten-year calibration period that I chose is most representative of the average discharge over the 1989-2013 period that is suitable for calibration selection. Reported USGS discharge data before 1989 was adjusted by the agency to account for the new location so all data can be used congruently and is suitable for validation of the DHSVM calibration.

Simulated model accuracy was measured by the Nash-Sutcliffe efficiency (NSE) (Nash and Sutcliffe, 1970), which compares daily mean observed streamflow (O) to simulated daily mean streamflow (P).

$$\boldsymbol{NSE = 1.0 - \frac{\sum_{i-1}^{n}(O_i - P_i)^2}{\sum_{i-1}^{n}(O_i - \bar{O}')^2}} \quad (2)$$

Additional statistically tests were evaluated based on the calibration guidelines of Moriasi et al. (2007, 2015). Besides NSE, I examined Pearson's coefficient of determination (R^2), percent bias (PBIAS), and root mean square error standard deviation ratio (RSR) to compare simulated and observed data. Each test compares the observed to the predicted data. R^2 is a measure of variance in the dependent variable that is explained by the independent variable, RSR is a measure of the standard deviation within the data, and PBIAS is the percent bias of the data. Based on Moriasi et al. (2007, 2015), performance evaluation criteria (PEC) of Very Good, Good, Satisfactory, and Not Satisfactory were used as model performance indicators, with my aim being to achieve at least a "Satisfactory" result for each statistical recommendation.

In addition to adjusting parameters to improve the statistical results of the full ten-year calibration time frame, I prioritized improving the statistical results of daily mean flows only in the May-September months when the streamflow is the lowest and when stream temperatures the warmest. I also examined Snow Water Equivalent (SWE) maps of the basin output by DHSVM and compared them to observed regional SWE. I also output the mean April 1 SWE at every cell in the North Fork basin over the calibration period and, extracted all the cells that fell within +/- 50 m of the Skookum Creek SNOTEL (SNOwpack TELemetry) station elevation (1009 m). The mean of these data was compared to observed mean of April 1 SWE at the Skookum Creek

SNOTEL. The Skookum Creek SNOTEL is about 80 km southeast of the centroid of the North Fork basin. It was chosen as a comparable proxy because it is also on the west side of the Cascades, removed from Cascade volcanoes that could alter the local weather, and at lower elevation than surrounding SNOTELS which make it a better approximation to conditions in the relatively low elevation North Fork basin.

After the statistical standards were met and suitable basin-wide SWE was achieved, I validated the calibrated DHSVM with a longer historical time series at the USGS gauge (Figures 1—2; 1983-2002).

2.4 Estimation of Mohseni and Leopold parameters

The RBM requires initial headwater conditions, which are estimated using a non-linear regression model that relates headwater temperature to air temperature as follows:

$$\boldsymbol{T_{head} = \mu + \frac{\alpha - \mu}{1 + e^{\gamma(\beta - T_{smooth})}}} \quad (3)$$

where α is an estimation of the maximum stream temperature (°C), β is air temperature at the inflection point of the function (°C), γ is the steepest slope of the function (ratio), and μ is the estimated minimum stream temperature (°C) (Mohseni et al., 1998). A smoothing parameter (T_{smooth}, unitless) is used to attenuate high frequency fluctuations in air temperature (T_{air}, °C) as follows:

$$\boldsymbol{T_{smooth} = \tau * T_{air}(t) + (1 - \tau) * T_{air}(t - 1)} \quad (4)$$

where,

$$\boldsymbol{\tau} = \frac{\mathbf{1}}{(\boldsymbol{smoothing\ period})} = \frac{\mathbf{1}}{(\mathbf{7}\ \boldsymbol{days} * \mathbf{8}\ \boldsymbol{timesteps\ per\ day})} \quad (5)$$

The Mohseni parameters were estimated with a least squares minimization algorithm using observed stream temperature measurements collected from the field and observed air temperature. Publicly available gridded climate data were used to estimate air temperature at sites in the basin where air temperature data were not available (PRISM Climate Group, 2017). During the summer of 2016, employees of the Stillaguamish Tribe Natural Resources Department installed 32 HOBO Onset TidbiT v2 water temperature data loggers with a 0.2 ^{o}C accuracy in various reaches throughout the North Fork Basin. The general installation methods of the US Environmental Protection Agency (Stamp et al., 2014) and Isaak et al. (2013) were followed, but an improved sensor mounting method was used to decrease the installation time and eliminate the use of an epoxy compound known to be harmful to aquatic species (Killebrew and Freeman, 2018). Of these 32 sites, the ten most upstream sensors were chosen to determine the Mohseni parameters for headwater conditions (Figure 2). The data loggers were visited to download the data and to check battery levels. Logger temperature datasets ranged between 6-14 months and included a temperature measurement every 30 minutes. Available gauge data from the WADOE Ciero gauge (decommissioned in 2012) and Oso gauge were also used in the Mohseni parameter calculations.

The RBM also requires Leopold parameters that are used to estimate stream velocity and depth for each stream segment in the basin using discharge values from the DHSVM. The parameters are used in relationships described by Leopold and Maddock (1953):

$$D = aQ^b \quad (6)$$

$$u = cQ^d \quad (7)$$

where Q is discharge (cms), u is velocity (m/s), D is depth (m), and a, b, c, and d are empirical constants. Field measurements of depth, width, and discharge were made at ten sites throughout the North Fork basin to estimate the empirical constants. Measurement sites occasionally corresponded with the temperature sensor locations (Figure 2). Stream discharge measurements were calculated at two different times during the summer of 2017 using the USGS stream gauging measurement technique (Turnipseed and Sauer, 2010). Care was taken to avoid times in late summer when headwaters could be dry. To determine discharge, measurements of stream depth and width was made with a wading rod and surveying measuring tape, and stream velocity was measured with a FlowMate 2000 flow meter. Minimum stream speed and depth were estimated using measured values. Flow data from the USGS 12167000 gauge and the WADOE Oso and Darrington gauges were also included in the Leopold parameter calculations. The Mohseni parameters and the Leopold parameters were adjusted to maximize the calibration efficiency of the model.

2.5 RBM Stream Temperature Calibration

The RBM is semi-Lagrangian, one-dimension model that is scalable in space and time (Yearsley, 2009, 2012; Sun et al., 2014). Initiated by headwater temperatures, the model tracks parcels of water through the river basin and estimates stream segment temperatures using heat exchanges from net solar radiation, net longwave radiation, sensible heat flux, latent heat flux, groundwater, and advected heat from adjacent tributary segments that are produced by the

DHSVM. Many factors contribute to overall stream temperature including climate, snowmelt, flow rate, basin topography, channel morphology, and riparian vegetation (Yearsley, 2012; Sun et al., 2015). The RBM has been used to model stream temperatures in the PNW by Yearsley (2009, 2012), Sun et al. (2015), and Cao et al. (2016), and Truitt (2018).

The RBM was calibrated to eight water years (2005-2012) of historical stream temperature data from the WADOE Oso gauge (WADOE, 2018; Figures 1—2) using the NSE coefficient method (Nash and Sutcliffe, 1970), and the statistical guidelines outlined by Moriasi et al. (2007, 2015). Although stream temperature is not specifically included in the Moriasi et al. (2007, 2015) evaluations of criteria to measure hydrologic (as with the DHSVM) and water quality outputs, I used the "General" criteria (Moriasi et al., 2015) to determine PEC for RBM results.

The 7-day average daily maximum (7-DADMax) is the mean of the maximum daily temperatures over a 7-day period, and is used as a measure of consistent stream temperatures that may be detrimental to aquatic species (Mantua et al., 2010). Following Washington State water quality standards, I determined the number of observed and simulated days exceeding the 16 ^{o}C 7-DADMax temperature standard for core summer salmon habitat (WADOE, 2017). During the calibration process, I tried to match observed versus simulated percent of days exceeding this threshold. In addition, the NSE and other statistical standards were examined in the May-September months to ensure reasonable model fit in the warmest months. Validation was achieved by comparing model output with stream temperature data taken at the now-decommissioned Deer Creek DOE gauge (Figure 2; 2005-2010).

2.6 Forecasted Simulations

The calibrated DHSVM and RBM were used to simulate the hydrology and stream temperatures in the North Fork of the Stillaguamish River basin for water years 2008-2098. I forced DHSVM with forecasted data from 10 GCMs and two emission scenarios following the methods of Murphy (2016) and Truitt (2018) for a total of 20 climate simulations. The 10 GCMs were recommended by Rupp et al. (2013) as the most suitable for climate prediction in the PNW (Table 2). Two emission representative concentration pathways (RCP) were chosen as simulated climate scenarios. RCP 4.5 is a medium-low warming scenario associate with moderate anthropogenic climate action. RCP 8.5 is a high warming climate scenario associated with minimal anthropogenic action and continued high emissions. The 20 climate scenarios were statistically downscaled to the basin using a multivariate adaptive constructed analogs (MACA) technique trained by the Livneh et al. (2013) data used in the calibration (Abatzoglou and Brown, 2012). The MACA method of downscaling takes the coarse, horizontal resolution of the global models and applies it to spatial complexities of smaller regions while accounting for local weather variables such as rain shadows, humidity, and local winds (Abatzoglou and Brown, 2012). The MACA data were bias-corrected, processed for the required DHSVM inputs, and disaggregated to 3-hr time steps by the UW-CIG. The projected climate data are at the same resolution the Livneh nodes (historic climate data). Both can be seamlessly applied across the basin and through time.

Historical land cover grid simulations mimic tree growth in the basin, and the potential reclamation of forested lands. I ran a secondary set of forecasted simulations of DHSVM and RBM using the calibrated models and the 1883 forest cover grid and riparian inputs to compare

modern vegetation to pre-industrial conditions (Cao et al., 2016). All other variables remained unchanged from the calibrated models. Pre-industrial vegetation conditions represent the upper bounds of remediation potential of the basin and is used as a demonstrative tool.

2.7 Data Analysis

Climate trends are often defined as 30-year "normals" to ensure the capture of natural climate oscillations such as El Niños and La Niñas which occur on sub-decadal to decadal frequencies. As such, simulation results are generated and analyzed over 30-year intervals centered on the years 1996 (hindcast), 2025, 2050, and 2075. The results of these forecasts represent a range of potential streamflow and stream temperature trends that were statistically evaluated using R, an open-source software for statistical and graphical computations. I examined median flows, median SWE, and median stream temperatures. The 7-DADMax was determined and the number of days stream temperatures exceeded safe temperatures for salmonid spawning, rearing, and migration (16 ^{o}C) were counted and averaged over the 30-year normals. Any 7-DADMax temperatures exceeding 22 ^{o}C, the lethal threshold for adult salmon species, were reported. Daily maximum (1-DMax) temperatures exceeding 17.5 ^{o}C are averaged and reported, as this is the salmon embryo lethality threshold (WADOE, 2017). My analysis followed, in part, the format of studies conducted in the near-by Nooksack River basin (Murphy, 2016; Truitt, 2018) in order to allow comparisons to the geographically similar South Fork Nooksack River.

To observe the change in temperature at individual stream segments from the hindcast to a future scenario, I compared mean temperatures in August, the hottest month of the year, at every stream segment between the hindcast and the 2075 centered 30-year normal using data from the

CSIRO-Mk3-6-0 GCM at the RCP 8.5 scenario, following the methods of Murphy and Rossi (2018). I repeated these simulations with the 1883 land cover and riparian conditions to determine which reaches have the potential to be most positively affected by improving the riparian conditions or vegetation cover.

3.0 Results

3.1 DHSVM Calibration

There are 42 Livneh nodes in and surrounding the North Fork basin that contain the historical meteorological time series used as input to the DHSVM. Although the time series at each Livneh node were biased corrected by the UW-CIG to account for orographic effects produced by variability in topography, the time series at any given location can still be unrealistic. Bias corrected data imposes temperature and precipitation lapse rates to gridded data to account for variability in local topography, and it is possible that the 1/16-degree grid does not resolve the high elevation areas at the head of the watershed because of its rapidly changing relief (Guillaume Mauger, personal communication, 2018). To identify biased nodes, I plotted the precipitation and air temperature time series for individual Livneh nodes and grouped them based on elevation and spatial location. Once grouped, nodes that showed excessive variability based on elevation or location were discarded as outliers. I ran DHSVM simulations using combinations of the remaining node locations until the DHSVM produced reasonable streamflow magnitudes and snow-water equivalent distributions. I eventually isolated five node locations that I used to further refine the calibration of the DHSVM (Figure 2).

Key DHSVM calibration parameters are the precipitation and air temperature lapse rates that can be defined as constant or vary by month; and the thickness and the vertical and lateral hydraulic conductivities of the soils in the watershed (Table 3). Again, I experimented with adjusting these until I achieved realistic simulated streamflow and a basin-wide SWE. The months that most effect the amount of snow available for melt and initial snow accumulation are

April and October, respectively. Adjusting the air temperature lapse rates in these months proved to be important for simulating the appropriate amount of snow accumulation (Table 3). Results from SWE comparisons between simulated output from the DHSVM and the Skookum Creek SNOTEL station showed good agreement. The Skookum Creek SNOTEL is at an elevation of 1009 m, about 80 km southeast of the North Fork basin. The average SWE on April 1 at the SNOTEL for the calibration period of 2002-2011 was 0.798 m. The average SWE on April 1 in the North Fork basin between 959-1059 m elevation was 0.758 m during the calibration period.

Streamflow calibration was achieved for water years 2003-2012 with an overall daily mean flow NSE of 0.55 and monthly NSE of 0.83, meeting the PEC standards of Satisfactory and Good (Figure 3; Table 4). The overall daily R^2 was 0.55 and monthly R^2 was 0.85, meeting Moriasi et al. (2015) guidelines of Not Satisfactory and Very Good, respectively. The lower overall daily R^2 result is likely the result of under-estimates of the winter peak flows. Because high stream temperatures are partially a result of low summer flows, I focused on improving statistical measures of model fit from May to September, resulting in daily mean NSE of 0.71 and R^2 of 0.65 that met PEC of Good and Satisfactory, respectively (Figure 3; Table 4).

The DHSVM validation was achieved by comparing simulated flow to observed flow from the USGS gauge (Figure 2) over twenty years of the hindcast period (1982 – 2001). The NSE of the overall daily mean streamflow was 0.54 and 0.52 in the summer months (Figure 4; Table 5), slightly less than those over the calibration period, but still meeting Satisfactory criteria. The monthly mean NSE and summer NSE met Good and Satisfactory criteria, respectively. Daily

mean R^2 values of 0.55 overall and 0.68 in May-September showed similar PEC results to the calibration period (Table 5).

3.2 RBM Calibration

To calibrate RBM, Mohseni parameters were calculated from the water temperature logger data (Figure 2) and PRISM Climate Group (2017) air temperature data, and manually adjusting the T_{smooth} and □ parameters (Table 6). The Mohseni parameters that were most impactful in the calibration were α and β. Truitt (2018) used Mohseni parameters from the highest elevation site for stream temperature calibration of the South Fork Nooksack River. I tried several parameters inputs including high elevation parameters, averages across parameters gained from loggers, gauges, and both. The selected T_{smooth} of 0.01 is similar that used by Truitt (2018) for the South Fork Nooksack (i.e., 0.018). Mantua et al. (2010) used the Mohseni regression method to estimate weekly stream temperatures across basin in the PNW and the α parameter used for the Stillaguamish River at the Arlington WADOE gauge (26.44 ^{o}C) is similar to the α parameter I use in this study (27.0 ^{o}C). During the spring and early summer when snowmelt was highest, the Mohseni method over estimated stream headwater temperatures, which produced warmer stream temperatures than observed values at the Oso gauge. As such, I invoked a snowmelt algorithm in the RBM similar to that applied by Truitt (2018). The algorithm uses the basin-average snowmelt output from the DHSVM. When the average basin snowmelt reached a predefined magnitude (0.0002 m^3/3hrs) the RBM snowmelt algorithm fixed headwater temperatures to 7 ^{o}C.

I experimented with Leopold parameter magnitudes, and ultimately used average values from my field discharge measurements and the USGS and WADOE gauges. The calibration improved

using minimum stream depth and speeds of 1.0 m and 1.0 m/s, respectively, through the whole basin (Table 6).

I achieved RBM calibration with an overall daily mean NSE of 0.83, and R^2 of 0.85, both with PECs of Very Good (Figure 5; Table 7). Monthly mean NSE of 0.90 and R^2 of 0.91 also met Very Good criteria. The May and September daily mean NSE of 0.58 and R^2 of 0.65 met PEC of Satisfactory. I assessed the fit of extreme stream temperatures by comparing the mean number of days per year over the calibration period that are over the 7-DADMax threshold temperature of 16 ^{o}C between the observed (57) and predicted (45).

During the calibration process, sensitivity tests were run on the main riparian inputs to the RBM: tree height, buffer width, and LAI. Sensitivity tests were run at the WADOE Oso gauge which is a low order, wide stream channel described by Sun et al. (2014) to be most influenced by improving riparian conditions due to the solar gain that these channels can experience. All these parameters were found to have an inverse relationship with temperature where increases in the parameters caused decreases in stream temperature. For example, decreasing LAI by an order of magnitude caused the stream segment to experience an average of 15 more days per year exceeding the 16 ^{o}C 7-DADMax threshold (Table 8). Consistent with sensitivity tests conducted by Sun et al. (2014), tree height values greater than 30 m did not decrease stream temperature much. Similarly, increasing the buffer width to more than 10 m had negligible effects on lowering stream temperature. Sun et al. (2014) also tested the bank to canopy distance and found that stream temperature decreased with decreased bank to canopy distance. The canopy overhang coefficient was not tested in this study, however increased overhang increases decreases the solar gain to the stream and likely decreases stream temperature.

Validation of RBM was achieved by comparing the observed streamflow at the Deer Creek WADOE gauge (Figure 6; 2005-2010). Validation results achieved Satisfactory or better standards (Table 9), despite summer temperatures generally being underestimated (Figure 6). Validation had an overall daily mean NSE of 0.80, and R^2 of 0.83, both meeting PEC of Very Good. The daily mean stream temperature in the summer months had a NSE of 0.50 and a R^2 of 0.60 (Figure 6; Table 9).

An anomalous year (2011) shows higher stream temperatures than expected during model calibration (Figure 5). I investigated different possibilities to account for this; for example, I validated the observed stream temperature trends in the North Fork Oso gauge with observed stream temperature in the South Fork Stillaguamish. I also determined that the DHSVM air temperature inputs followed the same trends as the observed stream temperature in 2011. I suspect it is related to isolated snowmelt in high-relief basins. Despite the unexplained anomaly, I still achieve PEC calibration standards (Table 7).

3.3 Forecasted Hydrology

Simulated streamflow at the USGS stream gauge over the 30-year hindcast period (1982-2011) peaked in November and decreased slightly through the winter (Figure 7; Table 10). Streamflow increased in the late spring with a second peak in May and decreased sharply through the months of July and August with lowest mean monthly flows in September. Through the 21st century, 30-year intervals, or "climate normals", centered on the years 2025, 2050, and 2075 were compared to historical medians. Simulated streamflow magnitudes generally increased in the fall and winter and decreased through the spring and summer with lowest

summer flows still occurring in September by the 2075 climate normal under RCP 8.5 conditions. The median projected flow of RCP 4.5 and 8.5 in the 2025 climate normal had a similar trend to the hindcast with peak flows in November, but slightly less than historic flow through the spring and summer. By the 2075 climate normal, the median of RCP 8.5 showed higher peak flows and lower low flows than that of the median RCP 4.5 scenario (Figure 7; Table 10).

SWE decreased sharply into the 21st century, with the lowest values of median daily SWE present in the RCP 8.5 scenario by the 2075 climate normal (Figure 7). The timing of peak SWE shifted from around April 1 for the hindcast, to around February 15 by the 2075 climate normal (Figure 7). Mapped output of the average April 1 SWE extent in the basin illustrates a recession of snow into the highest portions of the basin by the 2075 climate normal (Figure 8).

Modeling with the 1883 land cover altered the hydrology slightly. Generally, winter peaks were slightly less than the 2011 land cover results, and summer flows slightly more. By the 2075 climate normal, 1883 land cover resulted in a 4% decrease in median December flow for RCP 4.5 and a 6% decrease in median December flow for RCP 8.5. In the 2050 and 2075 climate normals, September flow is slightly lower under the 1883 land cover scenario than the 2011 land cover scenario for both RCPs (Table 11).

3.4 Forecasted Stream Temperature

Simulated stream temperature at the WADOE Oso gauge over the 30-year hindcast (1982-2011) displayed minimum median monthly temperatures in January (4.2 ^{o}C) and median monthly temperatures peaks in August (15.2 ^{o}C; Figure 9; Table 12). By the 2025 climate

normal, monthly median temperatures increased slightly, with June showing the largest increase. Stream temperatures continued to rise by the 2050 normal, with median temperatures above 16.0 ^{o}C in July and August for both RCP 4.5 and 8.5. By the 2075 normal, all median monthly stream temperatures were on average 0.9 ^{o}C higher for the RCP 8.5 scenario than for the RCP 4.5 scenario, and RCP 8.5 has median temperatures above 18.0 ^{o}C in July and August (Table 12). There was no significant shift in timing for peak temperatures throughout the 21st century as the peak temperatures consistently occurred between July and August (Figure 9). Snowmelt became less of an influence on stream temperature by the 2075 climate normal, as evidenced by the warmer spring and early summer stream temperatures compared to the hindcast (Figure 9; Table 11).

The hindcast at the WADOE Oso gauge averaged 32 days per year exceeding the 16.0 ^{o}C 7-DADMax threshold for core summer salmon habitat (Table 13). By the 2075 normal, the number of days per year exceeding the 7-DADMax threshold had increased close to 3 times for the RCP 4.5 scenario, and over 3.5 times for the RCP 8.5 scenario. I also examined the most extreme GCM, HadGEM2-ES under the RCP 8.5 emission scenario to test the upper bounds of threshold exceedance. Over a third of the year experiences stream temperatures above the 16.0 ^{o}C under this GCM by the 2075 climate normal (Table 13). The 7-DADMax reaches lethal temperature (22 ^{o}C) for adult salmon in 2069 under this extreme climate scenario, but lethal conditions are not met in the RCP 4.5 or 8.5 median scenarios. The 17.5 ^{o}C 1-DMax for salmon embryo lethality was exceeded an average of 8 days per year over the hindcast period, increasing 7.5 times under the RCP 4.5 and over 10 times under the RCP 8.5 scenario by the 2075 climate normal (Table 14).

Average August stream temperature increased in every stream segment throughout the basin between the hindcast and the 2075 climate normal using the CSIRO-Mk3-6-0 GCM under RCP 8.5 conditions. I chose this GCM as it represents the median stream temperature for the RCP 8.5 emission scenario in the 2075 climate normal (Figure 10). Individual segment temperature increases ranged from 2.6 ^{o}C to 6.2 ^{o}C. Basin-wide, stream segments increased an average of 4.8 ^{o}C (Figure 11). The same analysis was conducted using 1883 land cover and riparian values. Historical vegetation resulted in lower mean August stream temperatures by the 2075 climate normal at almost every stream segment when compared to the mean August temperatures by the 2075 climate normal under the modern land cover and riparian values. Restoring the basin to pre-industrial vegetation conditions decreased the mean August stream temperatures at individual stream segments as much as 1.6 ^{o}C, with an average decrease of 0.2 ^{o}C basin-wide. Although it is unlikely that the basin will be restored to land cover conditions similar to those in 1883, running these simulations verifies that impact of vegetation on stream flow and stream temperature (e.g., Table 8), and gives an upper bound of the change possible in the basin if re-forestation efforts were implemented.

4.0 Discussion

4.1 Forecasted Hydrology

Consistent with other regional forecast modeling studies of PNW rain-snow transient basins (e.g., Murphy, 2015), my results indicate streamflow into the 21st century in the North Fork Stillaguamish River increases in the winter months and decreases in the spring and summer as a result of a reduced snowpack. Historically, the basin streamflow peaks in the fall in response to increased rainfall and storm events, decreases in the winter when snowpack develops, peaks again in the spring as a result of snowmelt runoff, and slowly decays into the summer as precipitation decreases (Figure 7; Table 10). Through the 21st century, increased air temperatures caused the basin to transition to a rain-dominated basin. In the winter months more precipitation falls as rain rather than snow, which results in a reduced basin average SWE (Figures 7–8). The snowpack develops later in the season and melts out earlier. As a result, simulated streamflow magnitudes increased in the winter. Note that historic and forecasted median streamflows consistently decrease in December and rise again in January. The lower streamflows in December are in response to a distinct low-precipitation bias that is prevalent in the gridded Livneh data. Bias in the gridded data may result in lower runoff and rain-on-snow snowmelt (Figure 12). The December bias is also evident in the forecasted streamflow because the Livneh data were used to train the downscaled MACA data (Abatzoglou and Brown, 2012). While the December bias may effect forecasted snowpack and winter runoff, it will likely have little effect mid-to-late summer stream temperatures which are the focus of this study.

Streamflow magnitudes decreased through the spring and summer with less snowmelt sustaining summer flow and increased air temperatures causing drier summers (Figure 7; Table 10). Higher air temperatures in the RCP 8.5 scenario results in a highly reduced winter snowpack by the end of the 21st century, and no SWE supporting summer flow (Figure 7). The effects of climate warming on hydrology in the North Fork basin became more pronounced later in the century and with the RCP 8.5 scenarios. The above trends are consistent with forecasted simulations in the Nooksack River (Murphy, 2015), including the low streamflow trends in December because of the same biases in the gridded Livneh data (Figure 12). However, the forecasted winter streamflow in the North Fork Stillaguamish increased up to 63% through the 21st century (Table 10), while median winter flows forecasted in the Nooksack more than double.

Like previous modeling studies (e.g., Dickerson-Lange and Mitchell, 2014; Murphy, 2016), there are not large differences in streamflow and SWE between the RCP 4.5 and RCP 8.5 GCM scenarios during the first half of the 21st century (Figure 7; Figure 9). By the 2075 climate normal, streamflow and SWE trends vary more between the two emission scenarios. Though global greenhouse gas emissions are curbed under the RCP 4.5 scenario, the atmospheric concentrations of greenhouse gases do not stabilize until well into the 21st century (Hansen et al., 2005). From the present forward, any effects of either the acceleration or curbing of global emissions will likely not be fully realized until later in the 21st century.

The unusual geology of the North Fork Valley made calibrating the DHSVM challenging. The valley formerly drained the upper Skagit River, the upper Sauk River, and the Suiattle River before they were re-routed by the retreat of the Cordillean ice sheet and subsequent damming by lahars from near-by Glacier Peak (Booth et al., 2003, 2017). The present-day valley is wider

than most western Cascade river valleys and consists of unconsolidated alluvial and glacial deposits ranging from fine silt and clay glaciolacustrine sediments to coarser outwash gravels and till. The unconsolidated deposits store and discharge groundwater to the North Fork (Leonetti, 2015). Although the DHSVM accounts for groundwater input in to the streamflow system, the model initially under predicted low flows in the summer months, likely due to difficulties quantifying groundwater contributing to streamflow in the glacial deposits in the valley regions. To increase soil storage and groundwater input, I increased the maximum soil depth to 5 m and adjusted the soil vertical and lateral conductivities. Lower lateral conductivities delayed groundwater flow to streams and increased the spring and summer flows. I also increased snow accumulation in part to bolster summer streamflow for calibration. Consequently, my calibration may underestimate forecasted summer flow as the snowpack diminishes.

To increase simulated spring and summer streamflow to better match observed streamflow, I tried increasing the basin-wide SWE. Because of the lack of SNOTEL stations in the North Fork basin, I used SWE data from nearby SNOTELs to gauge magnitudes in the basin. The lowest nearby SNOTEL, Skookum Creek, showed good fit with my model accounting for 94% of the average April 1 SWE at similar elevations in the North Fork basin. Other SNOTELs in the vicinity did not match my results as well, primarily because of their locations. The Lyman Lake SNOTEL is due east of the North Fork basin, but it is on the east side of the main east-west Cascades divide. This may make it unsuitable for comparison to a watershed that flows west. The Elbow Lake Station, while being lower in elevation than the Skookum Creek basin, is close to Mt. Baker, a Cascade volcano of 3286 m elevation. Mt Baker could cause more snow at

Elbow Lake than what I predicted in the North Fork Stillaguamish basin because of enhanced orographic precipitation. A SNOTEL station installed in the North Fork basin may improve calibration but calibrating to a single point is not as reliable as estimating a basin-wide SWE by matching the spring snowmelt runoff to the streamflow. Calibrating to snowpack extent from satellite imagery could be possible using the distributed method of Revuelto et al. (2018), but such a comparison is beyond the scope of my study.

Groundwater is expected to remain a source of input to the North Fork Stillaguamish River (Leonetti et al., 2015) and may increase in the future. Winter precipitation magnitudes are forecasted to be greater than historical magnitudes (Abatzoglou et al., 2013), meaning precipitation falling as rain in winter will be recharging aquifers to a greater extent or aquifers will reach saturation earlier. Groundwater contribution to the river could become increasingly important to the spring and summer streamflow. However, drier summers and an increase in evapotranspiration in the future could lower the summer groundwater levels. Georgiadis (2018) predicts that evapotranspiration in the Puget Sound will increase due to warming air temperatures, recession of snowpack, and growth of forests following logging impacts of the latter half of the 20th century. This increase in evapotranspiration could also be the reason that September streamflow is lower under the 1883 land cover scenario than the present-day scenario (Tables 9 and 10).

Mantua et al. (2010) predicts that the rain-snow transient basins of the Cascades such as the Stillaguamish will show the highest increases in 20-year flood returns in all the PNW. While flood frequency is a concern to water managers and property owners, the inability of my calibration of the DHSVM to properly capture winter peak flow suggests that it may be under-

predicting peak flow in future simulations. Despite the care given to the site selection process of Livneh sites, and the adjustment of precipitation and temperature lapse rates, there are still problems with the disaggregated meteorological data. The DHSVM under-estimates peak flows in the fall and winter, likely in part because of the disaggregation of daily precipitation into 3-hour time steps (Figures 3–4). Precipitation magnitudes of storm events are spread over a 24-hour period, so the water volume during precipitation events at individual time-steps is underestimated. Lower intensity rainfall results in less rapid runoff and lower peaks, resulting in lower daily NSE and R^2 statistics over the course of the calibration duration (Figures 3–4). Other modeling studies in the region (e.g., Dickerson-Lange and Mitchell, 2014; Murphy, 2016) also experience this under-estimation of peak flows. However, because stream temperature extremes occur during May-September, I focused my calibration on those months rather than on winter peaks (Figure 9; Table 12). A more in-depth peak flow analysis would be necessary in the Stillaguamish basin to quantify the increase winter flood risks. More winter rainfall and higher intensity storms will also increase the risk of mass wasting resulting in increased sediment transport to the river, further jeopardizing salmon habitat (Krosby et al., 2016; Knapp, 2018).

4.2 Forecasted Stream Temperature

Simulated stream temperatures at the WADOE Oso gauge increased into the 21st century in response to forecasted increasing air temperatures and changes in basin hydrology (Table 11). Warmer air temperatures at higher elevations will increase the initial headwater temperatures through the Mohseni relationship, which in turn are propagated downstream as the water gains heat, primarily from radiation and sensible heat fluxes. Warmer air temperatures have an effect in all months of the year (Table 12). The greatest increase in monthly median stream temperature

under both the RCP 4.5 and 8.5 scenarios is in June, likely due to the reduction in snowmelt buffering stream temperature during the late spring (Table 12; Figures 7–9). The warmest predicted stream temperatures are in the late summer months, in part due to warmer headwater temperatures, but also a result of lower stream discharges. Because of less snowmelt and summer precipitation in general in the 21st century, stream discharge wanes in the summer, resulting in slower moving and shallower water that is more responsive to heat inputs.

Forecasted increased year-round stream temperatures will cause additional stress to already endangered aquatic species such as Chinook salmon and Steelhead trout. Consistent high stream temperatures are known to cause disease, death, pose migration barriers, and otherwise negatively affect fish populations (Mantua et al. 2010). The Chinook salmon that use the stream in the warmest months are at highest risk to the effects of warming temperatures. My simulated trends show increasing temperatures exceeding WADOE fresh water quality thresholds for salmon embryo lethality and adult salmon summer habitat (Tables 12—13). Using the WADOE 7-DADMax adult salmon lethal standard of 22 ^{o}C, lethal temperatures were not reached under median RCP 4.5 or RCP 8.5 conditions. However, using the GCM with the most extreme air temperature warming (HadGEM2-ES and RCP 8.5) lethal temperatures were reached in the year 2066, with an average of 9 days per year during the 2075 climate normal exceeded. My results are comparable to habitat assessment modeling studies conducted in the Stillaguamish River (e.g., Mantua et al., 2010; Krosby et al., 2016). Mantua et al. (2010), forecasted lethal temperatures to adult salmon in the main stem Stillaguamish by the 2080s. Likewise, Krosby et al. (2016) categorize Chinook salmon as ‘Extremely Vulnerable’ by the 2080s due to their thermal sensitivity. Because the Mantua et al. (2010) and Krosby et al. (2016) studies used a

gauge along the main stem of the Stillaguamish, downstream of the North Fork and South Fork confluence, my results are likely consistent with their findings under median RCP 4.5 and 8.5 emission scenarios as stream temperatures will increase with distance from the headwaters. Similarly, the Cao et al. (2016) study found more than 50 days per year above a 7-DADMax of 20 ^{o}C by the 2050 climate normal, though they used the outlet of the mainstem Stillaguamish as their reference point.

The summer-run Chinook that inhabit the Stillaguamish mostly spawn between the Deer Creek outlet and Swede Heaven bridge and occupy these areas through the hottest months of the year (SIRC, 2005). Salmon populations are known to be adaptable to high stream temperatures by inhabiting cold deep pools on the order of several meters to tens of meters wide during the summer (SIRC, 2005). Stream temperature anomalies studied by Leonetti et al. (2015) using 2001 Infra-Red thermal mapping of the main stem of the North Fork river channel noted many areas along the stream channel where water temperatures were up to 2 ^{o}C colder than the stream segment immediately upstream. These sites were classified by the anomaly cause (e.g., confluence, groundwater input) and have been identified as cold-water refugia, suitable for salmon refuge from the time they enter the stream in the late spring and summer until they spawn in mid to late summer and early fall (summer-run Chinook). Compared to the whole Stillaguamish basin, including the lower main stem and the South Fork (Figure 1), the North Fork held more than half of the observed cold-water anomalies.

The coldest cold-water anomalies along the North Fork described by Leonetti et al. (2015) are related to groundwater seeps and springs, which are therefore underestimated or not fully captured by the DHSVM. As such, my forecasted summer stream temperatures may be higher

than what may occur. As discussed above, the groundwater contribution to the river may increase in the future as a result of increased winter precipitation, possibly resulting in increased spring and summer discharge to the river that would help maintain localized cold-water refugia for salmon. For example, in the summer of 2015, after a winter of average precipitation but minimal snow due to warm air temperatures, the Stillaguamish Tribe Natural Resources Department did not witness or receive reports of any salmon deaths in any life cycle stage (Jason Griffith, personal communication, 2018). This could be the result of above normal winter aquifer recharge from rainfall that sustained summer stream discharge and cooler stream temperatures in localized pools. Although isolated pools could remain cool, average stream temperatures may remain higher. Stream temperatures recorded at the Oso stream gauge since 2004 were highest in the summer of 2015 (WADOE, 2018). By determining which cold-water refugia pools are in areas at most risk to summer temperature increases (Figure 11), riparian restoration can be prioritized accordingly through the basin.

Improving land cover and riparian conditions also has the capacity to counteract warming stream temperatures. The stream segments where stream temperatures are most moderated by the 1883 vegetation conditions are generally the stream segments with little or no vegetation under the present-day scenario (Figure 13). Under the 1883 conditions, bare mountain tops and logged areas were given vegetation characteristics of old-growth Douglas Fir, and along the main stem valley, areas of grass or cropland were converted to mixed forest. Both scenarios resulted in a large decrease in forecasted mean August stream temperatures when compared to the forecasted mean August stream temperatures under present-day land cover. Localized improvement of riparian conditions resulting in decreased stream temperatures is consistent with

several observation-based reach-scale studies (e.g., Roth et al., 2010; Ryan et al., 2013). While areas above present-day tree line are not realistically going to develop forested land cover, the difference between bare ground and forested cover demonstrates the importance of vegetation cover in moderating stream temperature.

Many previous modeling studies used generalized riparian inputs (e.g., Cao et al., 2016; Sun et al., 2015). Because riparian cover is influential on stream temperature, using high-resolution lidar data to determine average tree height at every stream segment improved the accuracy in the identification of reaches at risk for elevated temperatures. While Cao et al. (2016) use a basin-wide tree height of 10 m and a constant LAI value, the lidar analysis indicates that the basin-wide average tree height within the riparian buffer zone was 15.7 m (Table 1). As a result, the prediction of 50 days per year over a 7-DADMax of 20 ^{o}C by the 2050 climate normal may be an overestimation. My results show <1 day per year over a 7-DADMax of 20 ^{o}C at the WADOE Oso gauge through the 21st century. Moreover, the Cao et al. results are for the outlet of the Stillaguamish River into the Puget Sound (Figure 1) which is about 50 km downstream of the WADOE Oso gauge. While stream temperature does increase with distance from the headwaters, some of the difference between the two predictions is because of the underestimation of tree height through the basin by Cao et al. Because this basin typifies rain-snow transitional watersheds common in the PNW, my method for riparian characterization (Appendix A) could be used to inform other modeling ventures in the region. Kate Clarke, a MS graduate student at Western Washington University, is currently applying my methods to the South Fork Stillaguamish Basin (Figure 1) to provide the Stillaguamish Tribe with a comprehensive analysis of the whole Stillaguamish River watershed.

4.3 Uncertainty and Model Limitations

Both the DHSVM and RBM models have limitations as to the extent of natural processes that they simulate. For example, RBM does not account for water turbidity which can increase absorb energy and increase stream temperatures. Additionally, while RBM does estimate inputs to stream temperature from the hyporheic zone of the stream where mixing of groundwater and surface water occurs, and where water is often cooler than the water at the stream surface (Conant, 2004), there is a lack of data needed to properly characterize this source. DHSVM does not account for vegetation growth over the simulation period which may cause the model to under estimate evapotranspiration and stream shading over time. Like any spatially distributed model, there are also limitations due to the resolution and accuracy of the spatial data used to define the basin characteristics at the scale of the North Fork basin.

There are also limitations in the available data used or estimated in this study, such as stream geometry, snowmelt timing, and the meteorological forcing data. Because of the complex topography of the PNW, high resolution historic and futuristic climate data are inherently imperfect in their computation. e.g., downscaling from low resolution, monthly GCM data to a localized grid scale at 3-hr time steps. Although the downscaled meteorological data are bias-corrected, not all biases can be accounted for (Climatology Lab, 2018). For example, a low-precipitation bias was discovered in the forecasted meteorological data (Figure 12), consistent with the results of Murphy (2016). Advances in developing and expanding these types of downscaled and disaggregated gridded meteorological datasets are in progress by the UW-CIG using outputs from the Weather Research and Forecasting regional climate model (Guillaume Mauger, personal communication, 2018). These historical and forecasted data have better-quality

precipitation magnitudes that will allow for an improved quantification and assessment of peak flows and peak temperatures in the basin. Although uncertainties exist in my modeling approaches, trends can be extracted using statistically summaries of many climate realizations that can inform water managers.

5.0 Conclusions

Forecasted modeling with the DHSVM indicates that increasing air temperatures predicted into the 21st century will cause significant decreases in precipitation falling as snow, leading to an increase in winter rainfall runoff and higher streamflows, and a decrease in SWE that results in lower spring and summer flows. The effects will be more pronounced later in the century, particularly with the RCP 8.5 scenarios. Greater winter runoff and streamflows will likely increase sediment loading to streams that will further endanger salmon habitat and increase flood risks, requiring a more in-depth peak flow analysis in the Stillaguamish basin. My calibration of the DHSVM may not fully capture the groundwater discharge to the main stem in the valley and thereby may underestimate forecasted summer flow as the snowpack diminishes into the 21st century. Given that summer discharge magnitudes have a large influence on stream temperatures, further exploration of forecasted groundwater recharge and the identification of localized groundwater discharge that supports cold-water refugia would benefit salmon restoration efforts.

Stream temperatures simulated with the RBM increase into the 21st Century and correlate to forecasted increased air temperatures and changes in basin hydrology. The greatest stream temperature increases are in late spring, related to the reduction of snowpack, and subsequent spring snowmelt runoff. The warmest stream temperatures occur in mid to late summer, and WADOE fresh water quality thresholds for salmon embryo lethality and adult salmon summer habitat will continue to be exceeded. Compared to historic conditions, there was up to a fourfold increase in days exceeding 16 ^{o}C 7-DADMax temperatures at the end of the century for the most extreme GMC scenario, putting at risk already endangered species such as Chinook salmon and

Steelhead trout. Lidar differencing in ArcGIS allowed characterization of the riparian conditions along stream segments improved prior modeling efforts in the Stillaguamish basin by more accurately capturing vegetation characteristics that effect stream temperature. As such, ArcGIS maps showing projected stream temperatures changes along segments will better inform watershed managers in their restoration efforts in the North Fork.

6.0 Works Cited

Abatzoglou, J.T., and Brown, T.J., 2012, A comparison of statistical downscaling methods suited for wildfire applications: International Journal of Climatology, v. 32, p. 772–780, doi:10.1002/joc.2312.

Abatzoglou, J.T., Rupp, D.E., and Mote, P.W., 2013, Seasonal Climate Variability and Change in the Pacific Northwest of the United States: Journal of Climate, v. 27, p. 2125–2142, doi:10.1175/JCLI-D-13-00218.1.

Bennett, N.D. et al., 2013, Characterising performance of environmental models: Environmental Modelling & Software, v. 40, p. 1–20, doi:10.1016/j.envsoft.2012.09.011.

Black, R.W., Haggland, A., and Crosby, G., 2003, Characterization of instream hydraulic and riparian habitat conditions and stream temperatures of the Upper White River Basin, Washington, using multispectral imaging systems: Water-Resources Investigations Report USGS Numbered Series 2003–4022, http://pubs.er.usgs.gov/publication/wri034022 (accessed May 2017).

Booth, D.B., Haugerud, R.A., and Troost, K.G., 2003, The geology of Puget lowland rivers: Restoration of Puget Sound rivers. University of Washington Press, Seattle, p. 14–45.

Booth, A.M., LaHusen, S.R., Duvall, A.R., and Montgomery, D.R., 2017, Holocene history of deep-seated landsliding in the North Fork Stillaguamish River valley from surface roughness analysis, radiocarbon dating, and numerical landscape evolution modeling: Journal of Geophysical Research: Earth Surface, p. 2016JF003934, doi:10.1002/2016JF003934.

Cao, Q., Sun, N., Yearsley, J., Nijssen, B., and Lettenmaier, D.P., 2016, Climate and land cover effects on the temperature of Puget Sound streams: Hydrological Processes, v. 30, p. 2286–2304, doi:10.1002/hyp.10784.

Climatology Lab, 2018, MACA Data Limitations: http://www.climatologylab.org/maca.html (accessed November 2018).

Conant, B., 2004, Delineating and quantifying ground water discharge zones using streambed temperatures: Ground Water, v. 42, no. 2, p. 243-257, doi: 10.1111/j.1745-6584.2004.tb02671.x.

Cuo, L., Beyene, T.K., Voisin, N., Su, F., Lettenmaier, D.P., Alberti, M., and Richey, J.E., 2011, Effects of mid-twenty-first century climate and land cover change on the hydrology of the Puget Sound basin, Washington: Hydrological Processes, v. 25, p. 1729–1753, doi:10.1002/hyp.7932.

Dickerson-Lange, S.E., and Mitchell, R., 2014, Modeling the effects of climate change projections on streamflow in the Nooksack River basin, Northwest Washington: Hydrological Processes, v. 28, p. 5236–5250, doi:10.1002/hyp.10012.

Diffenbaugh, N.S. et al., 2017, Quantifying the influence of global warming on unprecedented extreme climate events: Proceedings of the National Academy of Sciences, v. 114, p. 4881–4886, doi:10.1073/pnas.1618082114.

Elsner, M.M., Cuo, L., Voisin, N., Deems, J.S., Hamlet, A.F., Vano, J.A., Mickelson, K.E.B., Lee, S.-Y., and Lettenmaier, D.P., 2010, Implications of 21st century climate change for the hydrology of Washington State: Climatic Change, v. 102, p. 225–260, doi:10.1007/s10584-010-9855-0.

Georgiadis, N., 2018, Are low flows changing in Puget Sound streams? University of Washington Puget Sound Institute Encyclopedia of Puget Sound, 5 p., https://www.pugetsoundinstitute.org/2018/08/are-low-flows-changing-in-puget-sound-streams/ (accessed October 2018).

Isaak, D., Horan, D., and P Wollrab, S., 2013, A Simple Protocol Using Underwater Epoxy to Install Annual Temperature Monitoring Sites in Rivers and Streams: Rocky Mountain Research Staion-General Technical Report-314.

Killebrew, K., and Freeman, K., 2018, Additional methods for conducting year-round, in-situ stream temperature monitoring: https://pnwclimateconference.org/posters.html (accessed October 2018).

Kim, S., McGaughey, R.J., Andersen, H.-E., and Schreuder, G., 2009, Tree species differentiation using intensity data derived from leaf-on and leaf-off airborne laser scanner data: Remote Sensing of Environment, v. 113, p. 1575–1586, doi:10.1016/j.rse.2009.03.017.

Knapp, K., 2018, The Effects of Forecasted Climate Change on Mass Wasting Susceptibility in the Nooksack River Basin [Master's Thesis]: Western Washington University.

Krosby, M., Morgan, H., Case, M., and Whitely Binder, L., 2016, Stillaguamish Tribe Natural Resources Climate Change Vulnerability Assessment: Climate Impacts Group, University of Washington, https://cig.uw.edu/news-and-events/publications/stillaguamish-tribe-natural-resources-climate-change-vulnerability-assessment/ (accessed December 2018).

Leach, J.A., Olson, D.H., Anderson, P.D., and Eskelson, B.N.I., 2016, Spatial and seasonal variability of forested headwater stream temperatures in western Oregon, USA: Aquatic Sciences, p. 1–17, doi:10.1007/s00027-016-0497-9.

Leonetti, F.E., 2015, Stillaguamish watershed baseflow analysis; 1911-2013: https://snohomishcountywa.gov/ArchiveCenter/ViewFile/Item/5917.

Leonetti, F.E., Terpstra, K., and Dittbrenner, B., 2015, Temperature anomalies in the Stillaguamish river mapped from 2001 thermal infrared aerial imagery: doi:10.13140/RG.2.1.1636.9129.

Leopold, L.B., and Maddock, T., 1953, The Hydraulic Geometry of Stream Channels and Some Physiographic Implications: U.S. Government Printing Office, 68 p.

Littell, J.S., Elsner, M.M., Whitely Binder, L.C., and Snover, A. (Eds.), 2009, The Washington Climate Change Impacts Assessment: Evaluating Washington's Future in a Changing Climate - Executive Summary, *in* The Washington Climate Change Impacts Assessment: Evaluating Washington's Future in a Changing Climate, Seattle, Washington, Climate Impacts Group, University of Washington, http://www.cses.washington.edu/db/pdf/wacciaexecsummary638.pdf (accessed March 2017).

Livneh, B., Rosenberg, E.A., Lin, C., Nijssen, B., Mishra, V., Andreadis, K.M., Maurer, E., and Lettenmaier, D.P., 2013, A Long-Term Hydrologically Based Dataset of Land Surface Fluxes and States for the Conterminous United States: Update and Extensions: Journal of Climate, v. 26, p. 9384–9392, doi:10.1175/JCLI-D-12-00508.1.

Mantua, N., Tohver, I., and Hamlet, A., 2010a, Climate change impacts on streamflow extremes and summertime stream temperature and their possible consequences for freshwater salmon habitat in Washington State: Climatic Change, v. 102, p. 187–223, doi:10.1007/s10584-010-9845-2.

Mantua, N., Tohver, I., and Hamlet, A., 2010b, Climate change impacts on streamflow extremes and summertime stream temperature and their possible consequences for freshwater salmon habitat in Washington State: Climatic Change, v. 102, p. 187–223, doi:10.1007/s10584-010-9845-2.

Mauger, G., Lee, S., Bandaragoda, C., Serra, Y., and Won, J., 2016, Refined Estimates of Climate Change Affected Hydrology in the Chehalis Basin: Report prepared for Anchor QEA, LLC. Climate Impacts Group, University of Washington, Seattle. doi, v. 10.

Mohseni, O., Stefan, H.G., and Erickson, T.R., 1998, A nonlinear regression model for weekly stream temperatures: Water Resources Research, v. 34, p. 2685–2692, doi:10.1029/98WR01877.

Moriasi, D.N., Arnold, J.G., Van Liew, M.W., Bingner, R.L., Harmel, R.D., and Veith, T.L., 2007, Model evaluation guidelines for systematic quantification of accuracy in watershed simulations: Transactions of the ASABE, http://agris.fao.org/agris-search/search.do?recordID=US201300848936 (accessed October 2018).

Moriasi, D., Gitau, M., Pai, N., and Daggupati, P., 2015, Hydrologic and Water Quality Models: Performance Measures and Evaluation Criteria: Transactions of the ASABE (American Society of Agricultural and Biological Engineers), v. 58, p. 1763–1785, doi:10.13031/trans.58.10715.

Mote, P., Snover, A., Capalbo, S., Eigenbrode, S., Glick, P., Littell, J., Raymondi, R., and Reeder, S., 2014, Ch. 21: Northwest: Climate Change Impacts in the United States: The Third National Climate Assessment, JM Melillo, Terese (TC) Richmond, and GW Yohe, Eds., US Global Change Research Program, p. 487–513.

Murphy, R., and Rossi, C., 2018, Forecasted flow and temperature changes in fish-bearing streams of the Hood Canal and Strait of Juan de Fuca: Salish Sea Ecosystem Conference, https://cedar.wwu.edu/ssec/2018ssec/allsessions/181.

Nash, J.E., and Sutcliffe, J.V., 1970, River flow forecasting through conceptual models part I — A discussion of principles: Journal of Hydrology, v. 10, p. 282–290, doi:10.1016/0022-1694(70)90255-6.

Pacific Northwest National Laboratory (PNNL), 2018, Distributed Hydrology Soil Vegetation Model: https://dhsvm.pnnl.gov/.

Parker, G., Davis, M., and Moon Chapotin, S., 2002, Canopy light transmittance in Douglas-fir-western hemlock stands: Tree physiology, v. 22, p. 147–57, doi:10.1093/treephys/22.2-3.147.

PRISM Climate Group, 2014, Average Annual Precipitation (1981-2010), Washington: Oregon State University, http://prism.oregonstate.edu/projects/gallery_view.php?state=WA.

PRISM Climate Group, 2017, Data Explorer: Time Series Values for Individual Locations: http://prism.oregonstate.edu/explorer/.

Puget Sound Indian Tribes, and Washington Department of Fish & Wildlife (PSIT & WDFW), 2017, Comprehensive Management Plan for Puget Sound Chinook: Harvest Management Component: 338 p., https://wdfw.wa.gov/publications/01947/ (accessed September 2018).

Revuelto, J. et al., 2018, Multi-Criteria Evaluation of Snowpack Simulations in Complex Alpine Terrain Using Satellite and In Situ Observations: Remote Sensing, v. 10, p. 1171, doi:10.3390/rs10081171.

Roth, T.R., Westhoff, M.C., Huwald, H., Huff, J.A., Rubin, J.F., Barrenetxea, G., Vetterli, M., Parriaux, A., Selker, J.S., and Parlange, M.B., 2010, Stream Temperature Response to Three Riparian Vegetation Scenarios by Use of a Distributed Temperature Validated Model: Environmental Science & Technology, v. 44, p. 2072–2078, doi:10.1021/es902654f.

Rupp, D.E., Abatzoglou, J.T., Hegewisch, K.C., and Mote, P.W., 2013, Evaluation of CMIP5 20th century climate simulations for the Pacific Northwest USA: Journal of Geophysical Research: Atmospheres, v. 118, p. 2013JD020085, doi:10.1002/jgrd.50843.

Ryan, D., Yearsley, J., and Kelly-Quinn, M., 2013, Quantifying the effect of semi-natural riparian cover on stream temperatures: Implications for salmonid habitat management: Fisheries Management and Ecology, v. 20, doi:10.1111/fme.12038.

Snohomish County Surface Water Management (SCSWM), 2015, Stillaguamish Temperature TMDL Adaptive Assessment and Implementation Project: Assessment Synthesis and Project Identification Report: Snohomish County Surface Water Management and Cardno, Inc. for Washington Department of Ecology, https://snohomishcountywa.gov/ArchiveCenter/ViewFile/Item/4301 (accessed November 2018).

Stamp, J., Hamilton, A., Craddock, M., Parker, L., Roy, A.H., Isaak, D.J., Holden, Z., Passmore, M., and Bierwagen, B.G., 2014, Best practices for continuous monitoring of temperature and flow in wadeable streams: EPA/600/R-13/170F. Washington, DC: U.S. Environmental Protection Agency, Office of Research and Development, National Center for Environmental Assessment, Global Change Research Program. 70 p., https://www.fs.usda.gov/treesearch/pubs/46926 (accessed August 2018).

Stillaguamish Implementation Review Committee (SIRC), 2005, Stillaguamish watershed Chinook salmon recovery plan: Snohomish County Department of Public Works, Surface Water Management, 187 p., https://www.snohomishcountywa.gov/Archive.asp?ADID=2163 (accessed March 2017).

Sun, N., Yearsley, J., Voisin, N., and Lettenmaier, D.P., 2015, A spatially distributed model for the assessment of land use impacts on stream temperature in small urban watersheds: Hydrological Processes, v. 29, p. 2331–2345, doi:10.1002/hyp.10363.

Truitt, S., 2018, Modeling the Effects of Climate Change on Stream Temperature in the Nooksack River Basin: WWU Graduate School Collection, https://cedar.wwu.edu/wwuet/642.

Truitt, S., Mitchell, R., Yearsley, J., and Grah, O., 2017, Calibration of a hydrologic and stream temperature model to the Nooksack River basin for climate change modeling:

Turnipseed, D.P., and Sauer, V.B., 2010, Discharge measurements at gaging stations: U.S. Geological Survey Techniques and Methods USGS Numbered Series 3-A8, http://pubs.er.usgs.gov/publication/tm3A8 (accessed May 2017).

United States Geologic Survey (USGS), 2017, USGS 12167000 NF Stillaguamish stream discharge data: https://waterdata.usgs.gov/wa/nwis/uv?site_no=12167000 (accessed May 2017).

Vano, J.A., Voisin, N., Cuo, L., Hamlet, A.F., Elsner, M.M., Palmer, R.N., Polebitski, A., and Lettenmaier, D.P., 2010, Climate change impacts on water management in the Puget

Sound region, Washington State, USA: Climatic Change, v. 102, p. 261–286, doi:10.1007/s10584-010-9846-1.

Wade, A.A., Beechie, T.J., Fleishman, E., Mantua, N.J., Wu, H., Kimball, J.S., Stoms, D.M., and Stanford, J.A., 2013, Steelhead vulnerability to climate change in the Pacific Northwest (A. Punt, Ed.): Journal of Applied Ecology, p. n/a-n/a, doi:10.1111/1365-2664.12137.

Washington State Department of Ecology (WADOE), 2008, Supplemental aquatic life temperature criteria information: http://www.ecy.wa.gov/Programs/wq/swqs/AquaticLifeTempSupp.html#beneuse (accessed January 2017).

Washington State Department of Ecology (WADOE), 2018, Gauge 05B090, North Fork Stillaguamish River stream monitoring at Oso data; https://fortress.wa.gov/ecy/eap/flows/station.asp?sta=05B090 (accessed November 2018).

Wigmosta, M.S., Vail, L.W., and Lettenmaier, D.P., 1994, A distributed hydrology-vegetation model for complex terrain: Water Resources Research, v. 30, p. 1665–1679, doi:10.1029/94WR00436.

Yearsley, J.R., 2012, A grid-based approach for simulating stream temperature: ResearchGate, v. 48, p. 1, doi:10.1029/2011WR011515.

Yearsley, J.R., 2009, A semi-Lagrangian water temperature model for advection-dominated river systems: Water Resources Research, v. 45, p. W12405, doi:10.1029/2008WR007629.

7.0 Tables

Table 1. Riparian conditions input in DHSVM for use in RBM temperature simulations, the method of parameter selection for the present-day vegetation conditions, and comparison to parameters used by Cao et al. (2016).

Parameter	Method	Description	Range	Cao value
Tree height	Computed for each individual segment with python script and ArcGIS	Lidar data were used to determine the average tree height in a 10 m buffer around each stream segment (Appendix A)	0 - 44 m (15.7 m basin-wide mean)	10 m
Buffer Width	Basin-wide average	Used sensitivity tests to determine and basin-wide estimation	10 m	5 m
Extinction Coefficient	Manual, based on LAI values of land cover file	In ArcGIS, I created extracted a land cover file that only contained cells that touched the stream file. I opened the attribute table and clicked through each segment, populating the rveg file with the appropriate monthly extinction coeff based on input values in the DHSVM configuration file.	0 - 0.13 (LAI equivalent of 0-8)	0.08 (LAI equivalent of 5)
Overhang Coefficient	Basin-wide average	This value was used by Cao et al (2016).	0.01	0.01
Canopy Bank Distance	Basin-wide average	This value was used by Cao et al (2016).	0 m	0 m
Channel Width	Manual, based on stream segment type	A value of 10 m was assigned to reaches along the main stem NF, a value of 5 m was assigned to all other segments.	5 m or 10 m	

Table 2. GCMs used to forecast meteorological inputs for both the RCP 4.5 and 8.5 scenarios, modified from Rupp et al. (2013).

Model	Center	Number of Ensemble Members: T/P/ Tmin/Tmax	Atmospheric Resolution (Lon. x Lat.)	Vertical Levels in Atmosphere
BCC-CSM1-1-M	Beijing Climate Center, China Meteorological Administration	3/ 3/ 3/ 3	1.12 x 1.12	26
CanESM2	Canadian Centre for Climate Modeling and Analysis	5/ 5/ 5/ 5	2.8 x 2.8	35
CCSM4	National Center of Atmospheric Research, USA	6/ 6/ 6/ 6	1.25 x 0.94	26
CNRM-CM5	National Centre of Meteorological Research, France	10/ 10/ 10/ 10	1.4 x 1.4	31
CSIRO-Mk3-6-0	Commonwealth Scientific and Industrial Research Organization/ Queensland Climate Change Centre of Excellence, Australia	10/ 10/ 10/ 10	1.8 x 1.8	18
HadGEM2-ES	Met Office Hadley Center, UK	5/ 5/ 5/ 5	1.88 x 1.25	38
HadGEM2-CC	Met Office Hadley Center, UK	1/ 1/ 1/ 1	1.88 x 1.25	60
IPSL-CM5A-MR	Institute Pierre Simon Laplace, France	3/ 3/ 1/ 1	2.5 x 1.25	39
MICROC5	Atmosphere and Ocean Research Institute (The University of Tokyo), National Institute for Environmental Studies, and Japan Agency for Marine-Earth Science and Technology	5/ 5/ 5/ 5	1.4 x 1.4	40
NorESM1-M	Norwegian Climate Center	3/ 3/ 3/ 3	2.5 x 1.9	26

Table 3. Notable DHSVM calibration parameters.

Description	Value
Minimum rain temperature threshold	1.0 ^{o}C
Maximum snow temperature threshold	1.0 ^{o}C
Snow water capacity	0.03
Temperature lapse rate	
Nov-Mar	-0.0055 ^{o}C/m
April and October	-0.0045 ^{o}C/m
May-September	-0.004 ^{o}C/m
Precipitation lapse rate	0.0003 m/m
Soil lateral conductivity	
Loamy sand	0.0005 m/s
Sandy loam	0.0008 m/s
Silt	0.001 m/s
Soil vertical conductivity	
Loamy sand	0.005 m/s
Sandy loam	0.001 m/s
Silt	0.005 m/s
Soil maximum depth	5 m
Soil minimum depth	0.76 m
Stream network source area	22000 m^2

Table 4. Performance evaluation criteria of the validation of DHSVM to streamflow measured at the USGS stream gauge (station 12167000) from water years 2003-2012.

	All data		**May - Sept only**	
	Daily mean	Monthly mean	Daily mean	Monthly mean
NSE	0.55	0.83	0.71	0.85
R-Squared	0.55	0.85	0.74	0.88
RSR *	0.67	0.41	0.63	0.39
PBIAS	8.46	8.41	8.84	0.80
PEC rating:	Very Good	Good	Satisfactory	Not Satisfactory

* Daily RSR criteria are not provided in Moriasi et al (2007). However, the other PEC included the same value ranges for both monthly and daily mean values, so it was assumed that the monthly ranges given by Moriasi et al. (2007) could be used as guidelines for daily criteria as well.

Table 5. Performance evaluation criteria of the validation of DHSVM to streamflow measured at the USGS stream gauge (station 12167000) from water years 1982-2001.

	All data		**May - Sept only**	
	Daily mean	Monthly mean	Daily mean	Monthly mean
NSE	0.54	0.78	0.52	0.61
R-Squared	0.55	0.78	0.68	0.87
RSR *	0.68	0.47	0.67	0.59
PBIAS	2.59	2.67	-25.96	-25.95
PEC rating:	Very Good	Good	Satisfactory	Not Satisfactory

* Daily RSR criteria are not provided in Moriasi et al (2007). However, the other PEC included the same value ranges for both monthly and daily mean values, so it was assumed that the monthly ranges given by Moriasi et al. (2007) could be used as guidelines for daily criteria as well.

Table 6. Mohseni and Leopold parameters used in the calibration of RBM and their source.

Parameter	Value	Source
Mohseni α	27.0 ºC	Adjusted
Mohseni β	13.3 ºC	Mean of field sites
Mohseni γ	0.2	Mean of field sites
Mohseni μ	0.8 ºC	Mean of field sites
Mohseni Smoothing	0.01 ºC	Adjusted
Leopold a	0.63	Mean of field sites and agency gauges
Leopold b	0.4	Mean of field sites and agency gauges
Leopold c	0.2	Mean of field sites and agency gauges
Leopold d	0.4	Mean of field sites and agency gauges
Leopold min depth	1.0 m	Adjusted
Leopold min speed	1.0 m/s	Adjusted

Table 7. Performance evaluation criteria of the calibration of RBM to stream temperature measured at the WADOE Oso gauge from water years 2005-2012.

	All data		**May - Sept only**	
	Daily mean	Monthly mean	Daily mean	Monthly mean
NSE	0.83	0.90	0.58	0.66
R-Squared	0.85	0.91	0.65	0.73
RSR *	0.42	0.32	0.64	0.57
PBIAS	-3.42	-3.43	-3.71	-3.72
PEC rating:	Very Good	Good	Satisfactory	Not Satisfactory

* Daily RSR criteria are not provided in Moriasi et al (2007). However, the other PEC included the same value ranges for both monthly and daily mean values, so it was assumed that the monthly ranges given by Moriasi et al. (2007) could be used as guidelines for daily criteria as well.

Table 8. Sensitivity tests of days exceeding 16 ºC 7-DADMax threshold over the 8-year calibration period (2005-2012) under different LAI (and corresponding extinction coefficient) conditions at the North Fork Stillaguamish WADOE Oso gauge and average days exceeding the 16 ºC 7-DADMax threshold per year.

LAI (Extinction Coefficient)	**Days exceeding**	**Average days per year**
0.5 (0.008)	435	54
5 (0.08)	292	36
50 (0.8)	199	25

Table 9. Performance evaluation criteria of the validation of RBM to stream temperature measured at the WADOE Deer Creek gauge from water years water years 2005-2012.

	All data		**May - Sept only**	
	Daily mean	Monthly mean	Daily mean	Monthly mean
NSE	0.80	0.86	0.50	0.56
R-Squared	0.83	0.90	0.60	0.68
RSR *	0.45	0.37	0.68	0.63
PBIAS	0.87	0.81	9.61	9.64
PEC rating:	Very Good	Good	Satisfactory	Not Satisfactory

* Daily RSR criteria are not provided in Moriasi et al (2007). However, the other PEC included the same value ranges for both monthly and daily mean values, so it was assumed that the monthly ranges given by Moriasi et al. (2007) could be used as guidelines for daily criteria as well.

Table 10. Modeled monthly median streamflow in cubic meters per second (cms) at the USGS gauge (station 12167000) in the North Fork Stillaguamish River for median GCM results over 30-years surrounding 2025, 2050, 2075, and the historic (hindcast) period.

Month	**Historic (cms)**	RCP 4.5	RCP 8.5	RCP 4.5	RCP 8.5	RCP 4.5	RCP 8.5
		2025		**2050**		**2075**	
January	51.0	63.6	71.7	79.1	78.8	80.7	88.2
February	44.5	52.0	55.0	57.2	60.7	63.9	71.2
March	45.9	58.2	57.7	61.4	61.9	62.8	63.7
April	56.9	61.1	60.7	60.0	61.6	58.3	52.5
May	67.3	54.4	52.7	42.8	43.1	37.1	30.0
June	46.9	33.6	32.2	25.7	24.6	21.2	16.9
July	19.9	14.4	14.1	11.3	10.7	10.0	8.7
August	9.5	7.5	7.3	6.2	5.9	5.9	5.2
September	8.4	6.6	6.9	6.0	5.4	5.4	5.1
October	27.1	22.4	23.6	24.2	20.7	24.1	23.2
November	76.3	76.5	79.8	74.2	81.7	90.5	86.8
December	52.6	62.0	66.2	76.7	76.9	80.7	92.2

Table 11. Modeled monthly median streamflow in cubic meters per second (cms) at the USGS gauge (station 12167000) in the North Fork Stillaguamish River under 1883 land cover and riparian conditions for median GCM results over 30-years surrounding 2025, 2050, 2075, and the historic (hindcast) period.

Month	**Historic (cms)**	RCP 4.5	RCP 8.5	RCP 4.5	RCP 8.5	RCP 4.5	RCP 8.5
		2025		**2050**		**2075**	
January	51.0	61.2	68.8	75.9	76.3	77.2	81.5
February	44.5	50.8	52.9	55.2	58.0	59.6	66.1
March	45.9	54.2	53.6	57.2	56.9	57.7	58.0
April	56.9	54.3	52.7	51.9	52.2	49.5	46.6
May	67.3	42.7	41.2	34.7	35.0	30.7	26.8
June	46.9	30.8	29.6	24.5	23.9	20.6	16.7
July	19.9	15.7	15.7	11.8	11.3	10.5	8.8
August	9.5	8.3	8.2	6.6	6.2	6.0	5.3
September	8.4	6.9	7.3	5.9	5.4	5.3	4.8
October	27.1	20.0	20.3	20.6	17.5	21.1	19.3
November	76.3	69.1	71.9	67.3	73.4	81.2	78.1
December	52.6	60.9	63.2	73.6	73.2	77.8	86.5

Table 12. Modeled monthly median stream temperature in degrees Celsius at the WADOE Oso gauge in the North Fork Stillaguamish River for median GCM results over 30-years surrounding 2025, 2050, 2075, and the historic (hindcast) period.

Month	**Historic °C**	RCP 4.5	RCP 8.5	RCP 4.5	RCP 8.5	RCP 4.5	RCP 8.5
		2025		**2050**		**2075**	
January	4.2	4.4	4.5	4.7	5.0	5.0	5.8
February	4.8	5.0	4.9	5.3	5.4	5.6	6.3
March	5.5	5.8	5.8	6.2	6.2	6.7	7.2
April	6.7	7.4	7.3	7.7	7.8	8.1	8.6
May	8.1	8.7	8.9	9.5	9.8	10.6	11.8
June	9.4	11.7	11.7	13.3	13.8	14.6	15.8
July	13.8	15.4	15.5	16.6	17.0	17.4	18.4
August	15.2	16.2	16.2	16.9	17.2	17.4	18.3
September	13.6	14.5	14.5	15.3	15.6	15.7	16.7
October	10.1	11.1	11.3	12.1	12.5	12.5	13.8
November	6.1	6.7	6.8	7.2	7.6	7.7	8.6
December	4.4	4.7	4.9	5.2	5.6	5.5	6.4

Table 13. Average days per year at the North Fork Stillaguamish WADOE Oso gauge exceeding 16 ^{o}C 7-DADMax temperatures per climate normal for each median RCP emission scenario and the GCM with most extreme climate projection, HadGEM2-ES (RCP 8.5).

Emission Scenario	Historic	2025	2050	2075
Moderate (RCP 4.5)	32	58	79	95
Severe (RCP 8.5)	32	59	88	117
GCM HadGEM2-ES (RCP 8.5)	32	68	97	136

Table 14. Average days per year at the North Fork Stillaguamish WADOE Oso gauge exceeding 17.5 ^{o}C 1-DMax temperatures per climate normal for each median RCP emission scenario and the GCM with most extreme climate projection, HadGEM2-ES (RCP 8.5).

Emission Scenario	Historic	2025	2050	2075
Moderate (RCP 4.5)	8	21	45	60
Severe (RCP 8.5)	8	24	56	87
HadGEM2-ES (RCP 8.5)	8	32	60	105

8.0 Figures

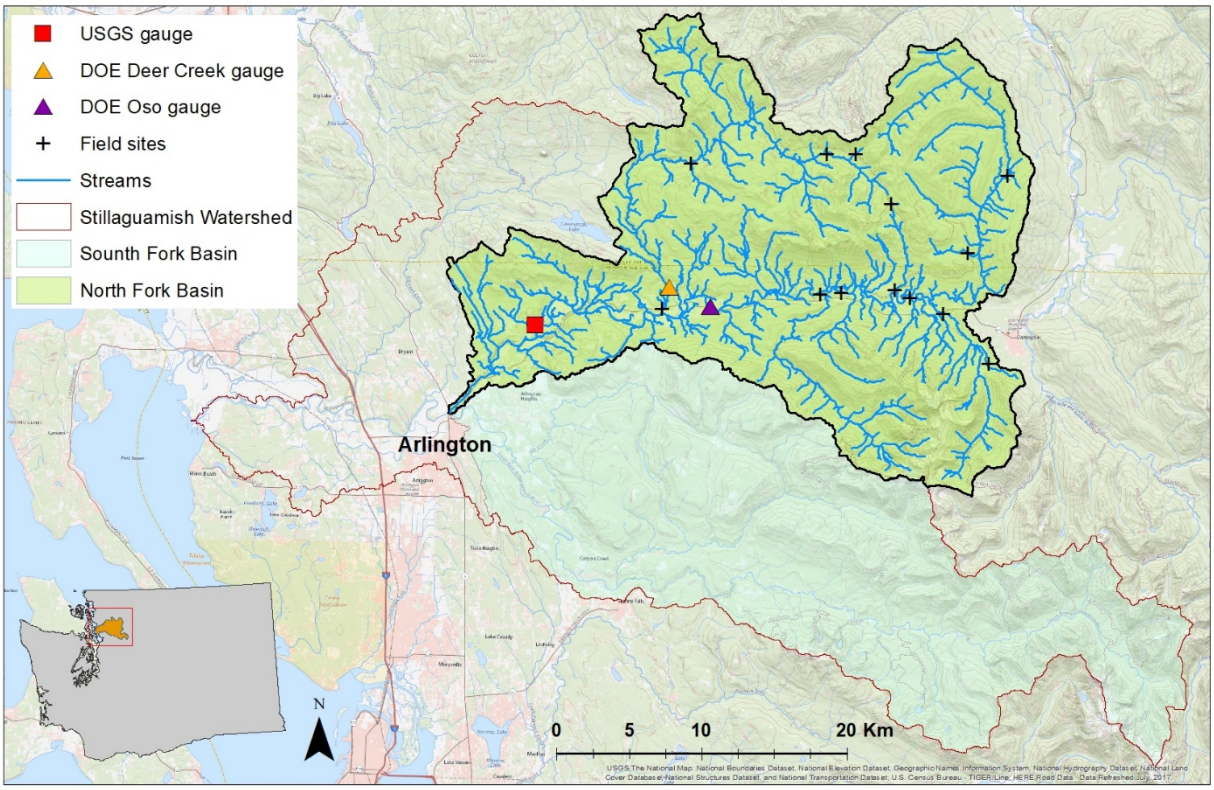

Figure 1. The Stillaguamish River basin (WRIA 5) in northwest Washington State, USA.

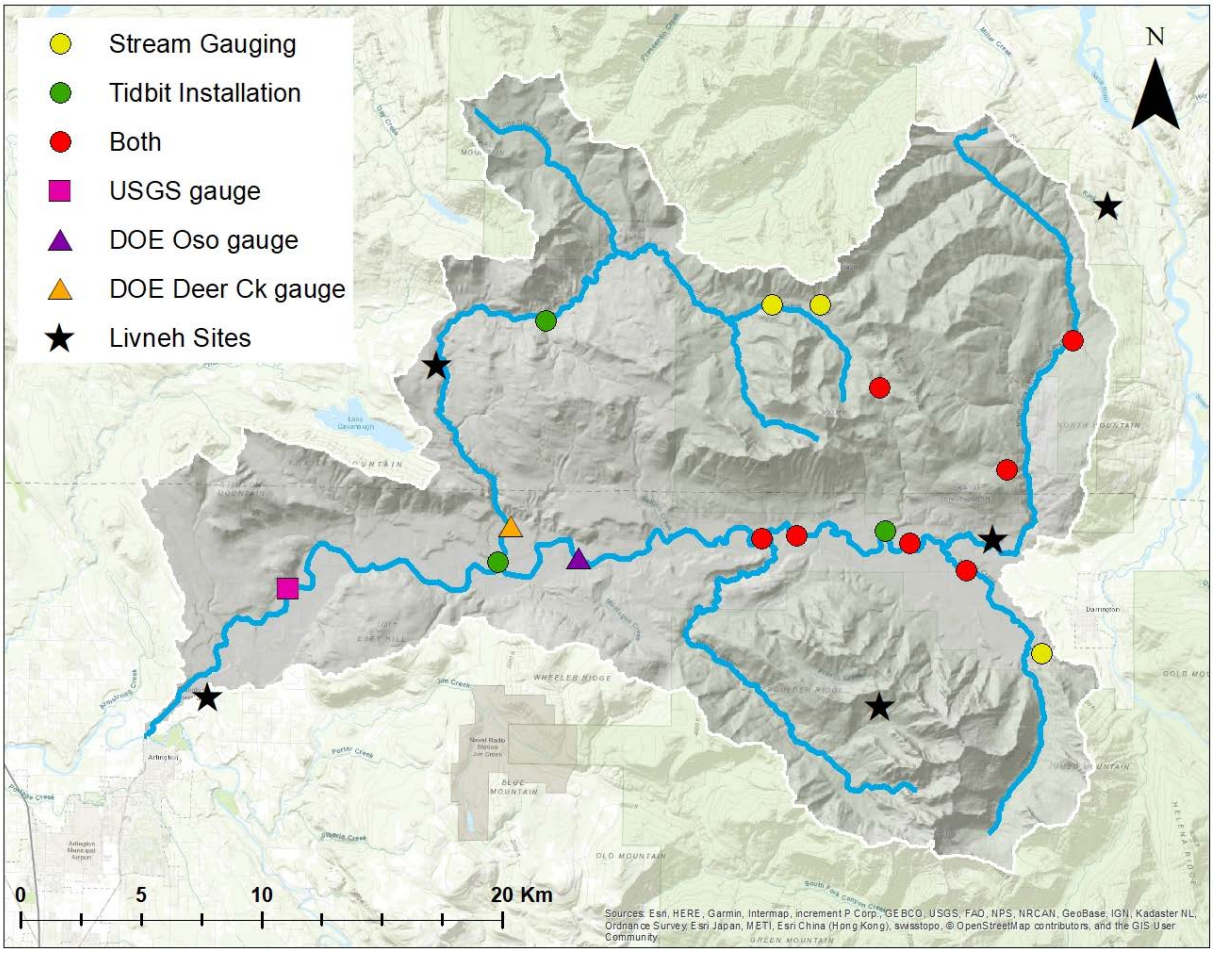

Figure 2. Field sites, agency stream gauges, and location of input sites for disaggregated meteorological data in the North Fork Stillaguamish River basin in northwest Washington State, USA.

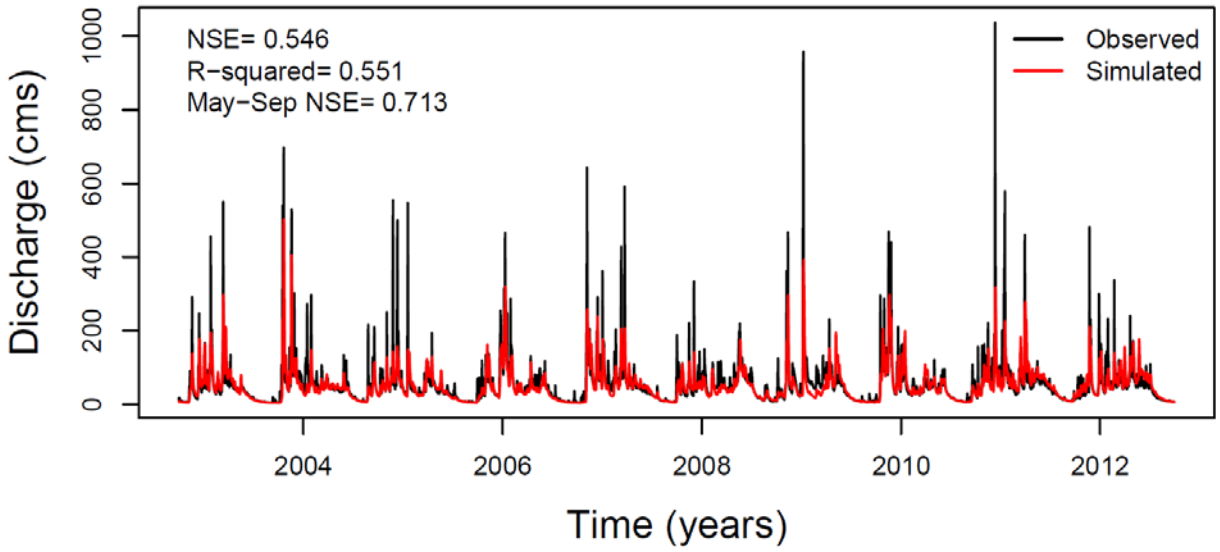

Figure 3. Calibration of the DHSVM to daily mean flow at the USGS stream gauge (station 12167000) over water years 2003-2012.

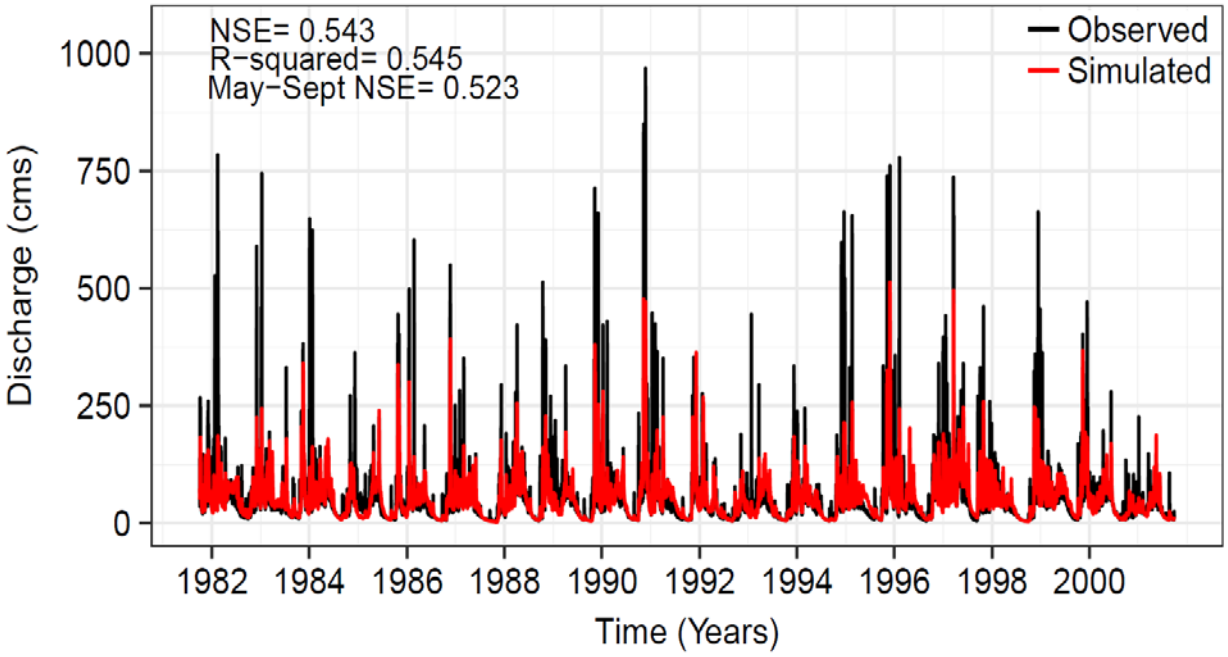

Figure 4. Validation of the DHSVM to daily mean flow at the USGS stream gauge (station 12167000) over water years 1983-2002.

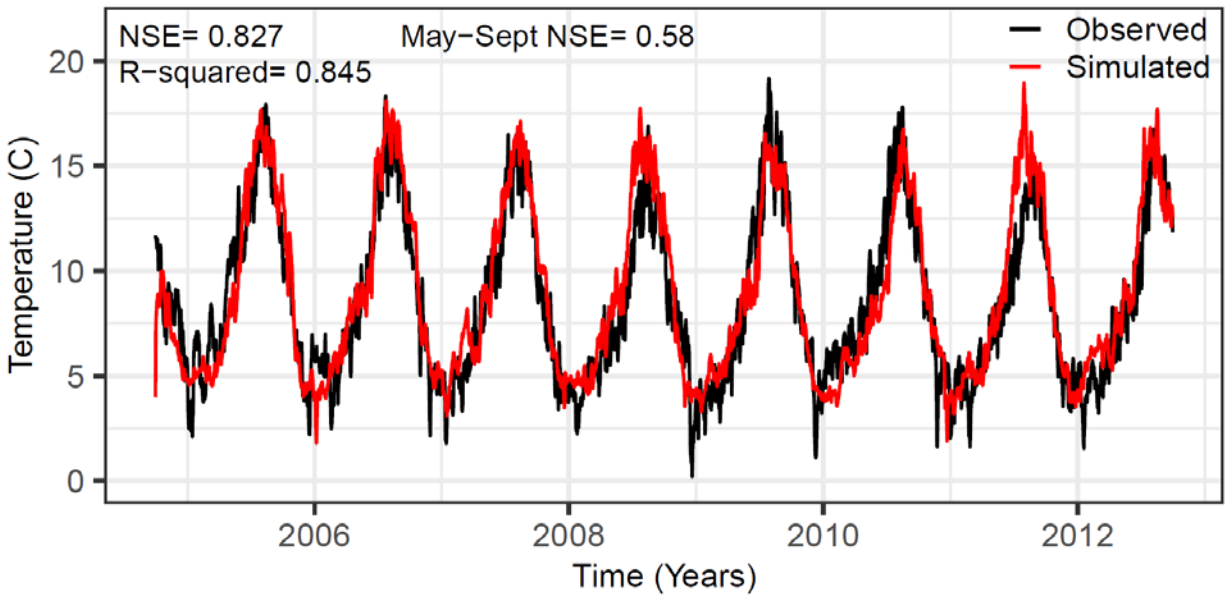

Figure 5. Calibration of the RBM to mean daily stream temperature at the WADOE Oso gauge over water years 2005-2012.

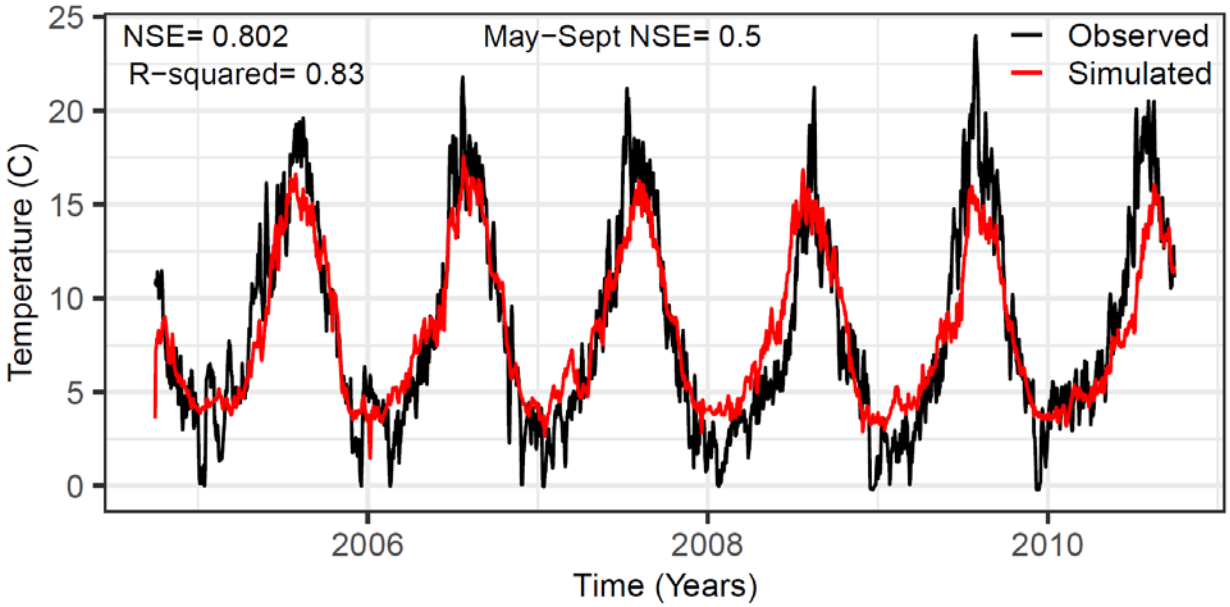

Figure 6. Validation of the RBM to mean daily temperature at the WADOE Deer Creek gauge over water years 2005-2010.

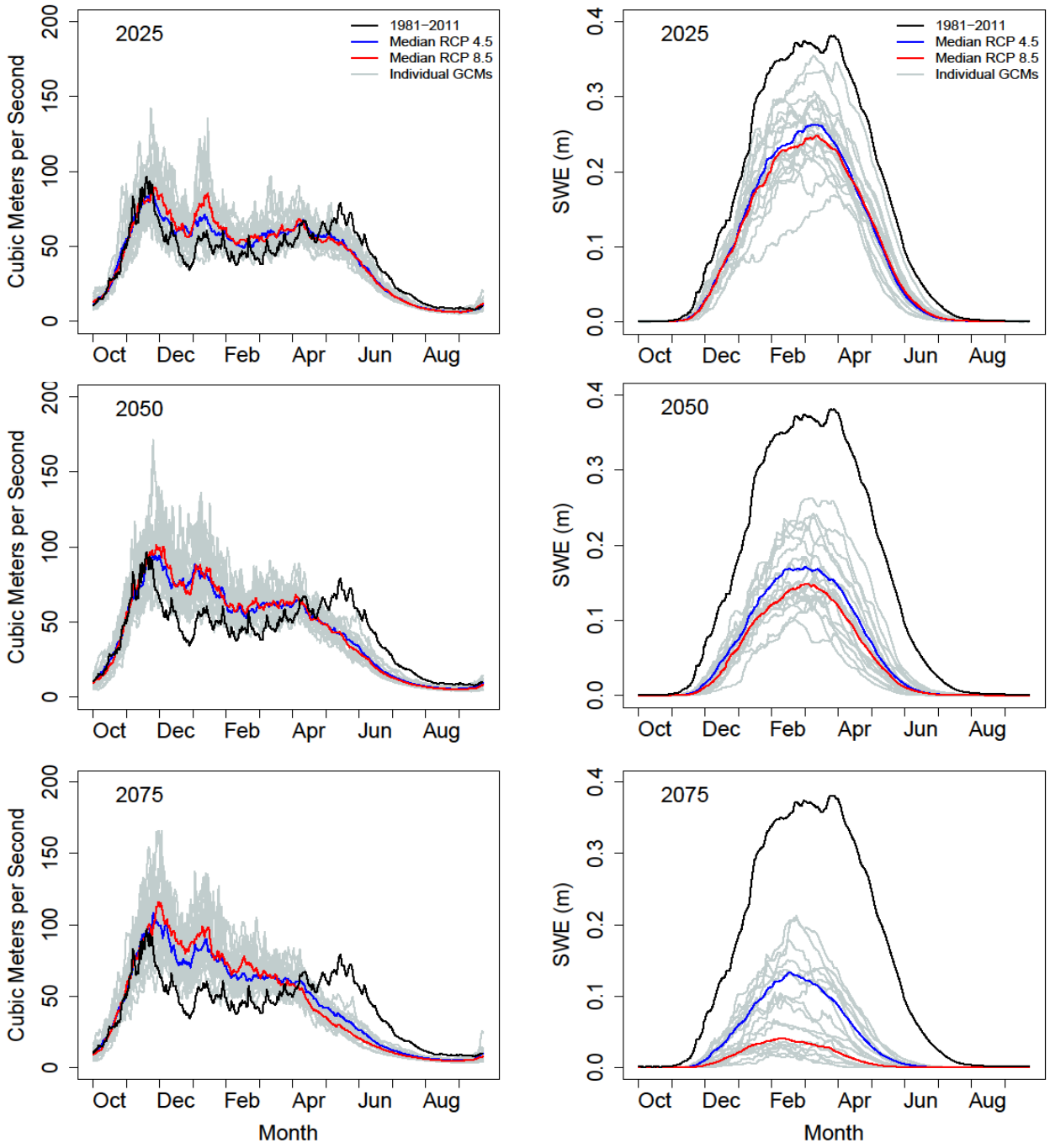

Figure 7. Monthly median streamflow and snow water equivalent over three 30-year climate normals centered on the years 2025, 2050, and 2075 at the USGS gauge. Median hindcast values (30-year climate normal centered on the year 1996) are represented by the black line, the median RCP 4.5 values as the blue line, the median RCP 8.5 value as the red line, and individual GCMs by the grey lines.

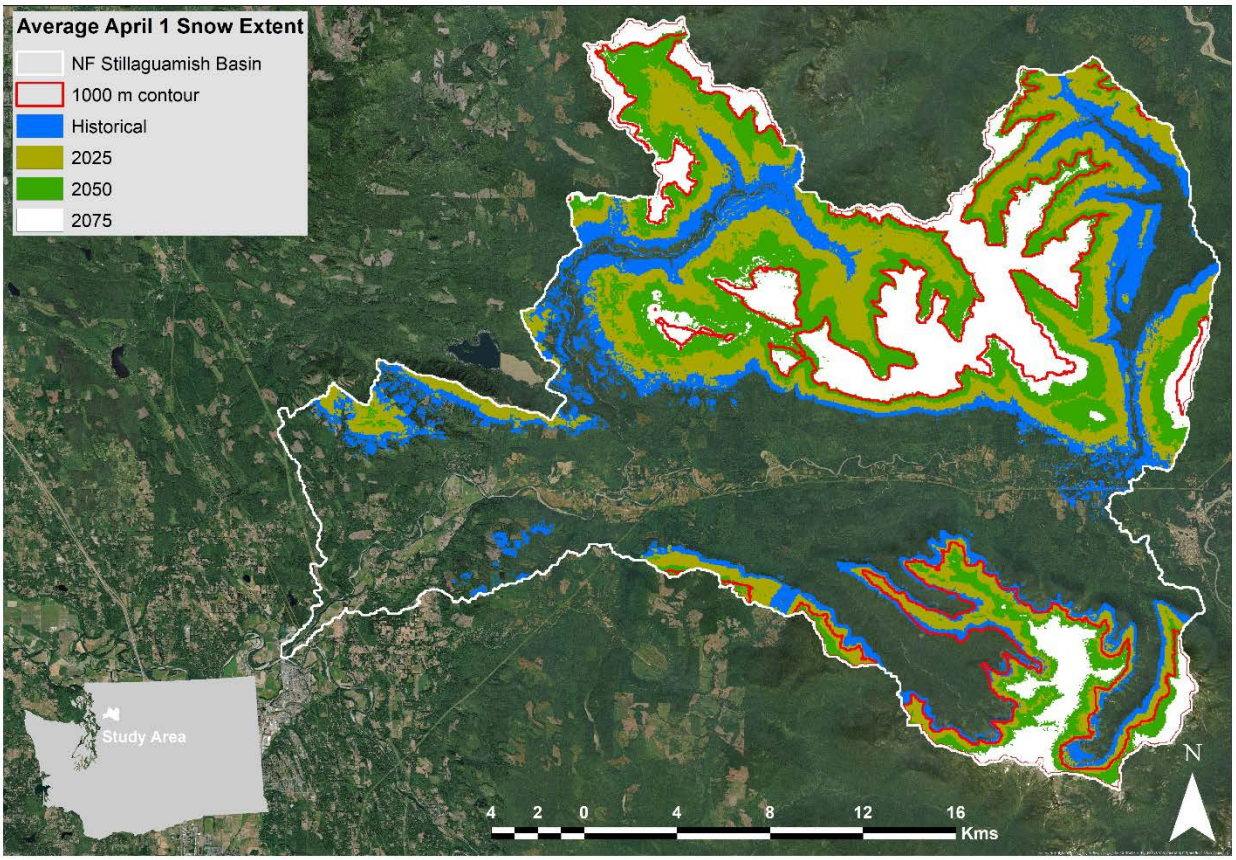

Figure 8. Average April 1 SWE extent over three forecasted 30-year normals in the North Fork Stillaguamish basin.

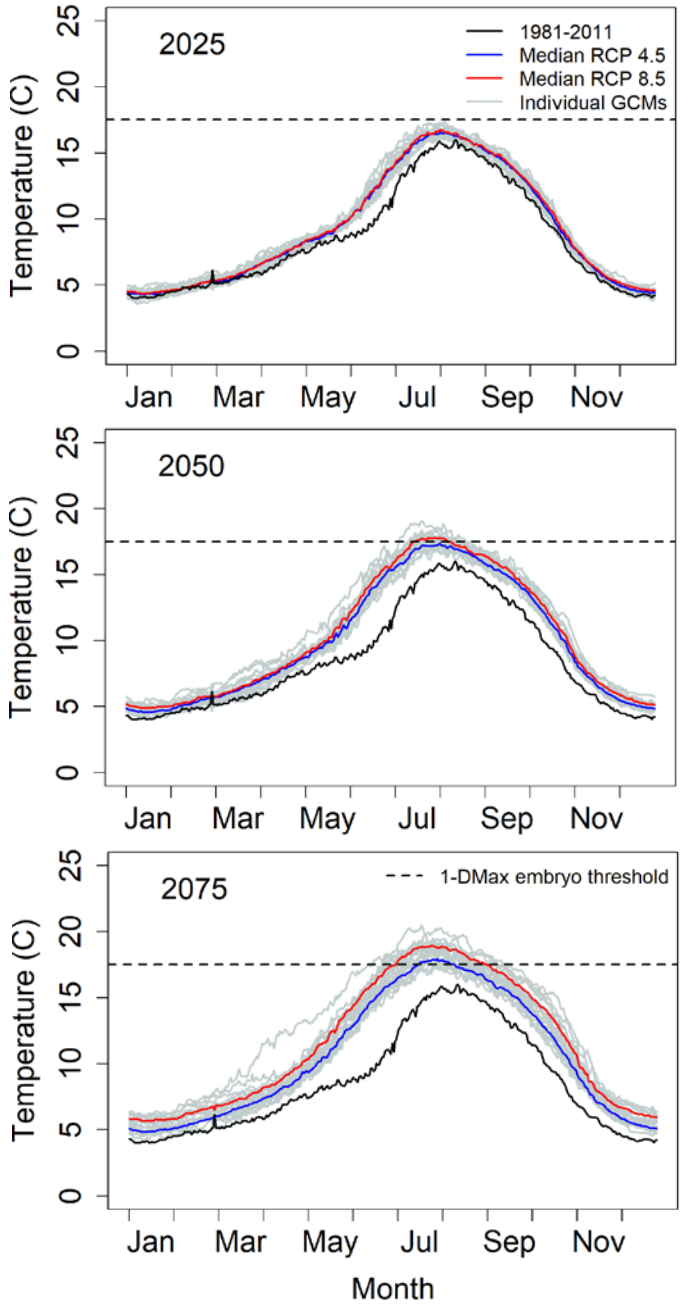

Figure 9. Monthly median stream temperature over three 30-year climate normals centered on the years 2025, 2050, and 2075 at the WADOE Oso gauge. Median hindcast values (30-year climate normal centered on the year 1996) are represented by the black line, the median RCP 4.5 values as the blue line, the median RCP 8.5 value as the red line, and individual GCMs by the grey lines. The horizontal dashed line represents the 1-DMax for salmon embryo mortality.

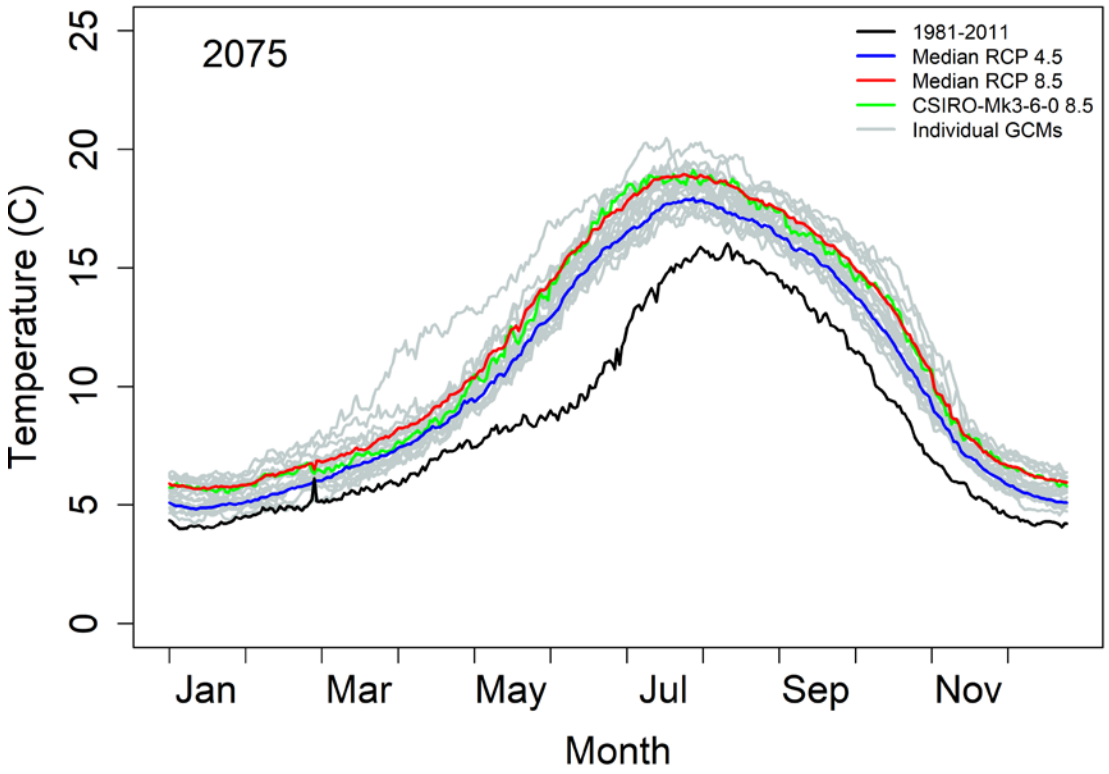

Figure 10. Verification that the CSIRO-Mk3-6-0 GCM under RCP 8.5 conditions (green line) is representative of the median of the 10 RCP 8.5 GCMs (red line) over the 30-year climate normal centered on 2075. The blue line is the median of the RCP 4.5 GCMs, the black line represents the hindcast, and the grey lines represent individual GCMs.

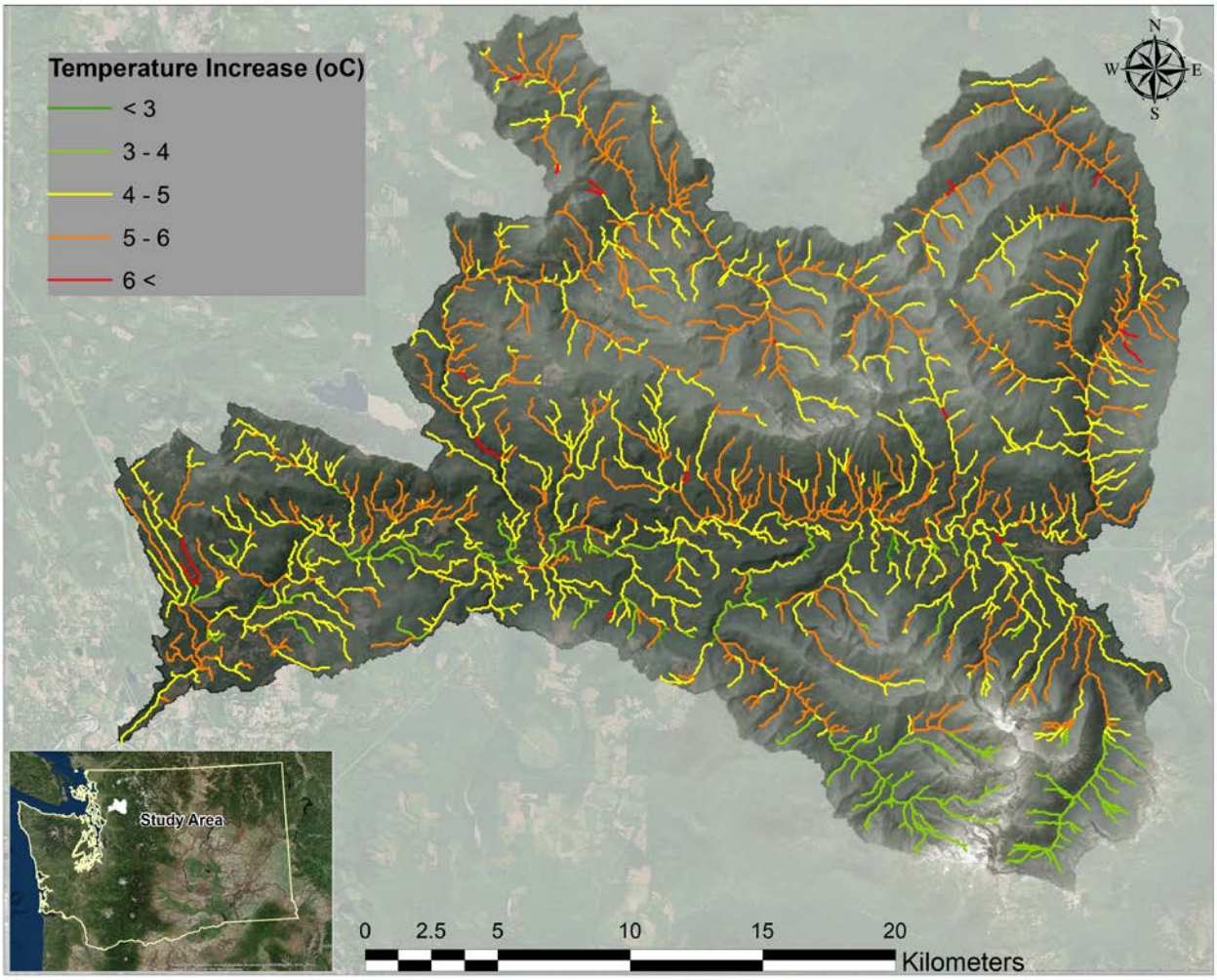

Figure 11. Average August stream temperature increase at every stream segment in the North Fork Stillaguamish River between the hindcast and the 2075 climate normal under CSIRO-Mk3-6-0 GCM and RCP 8.5.

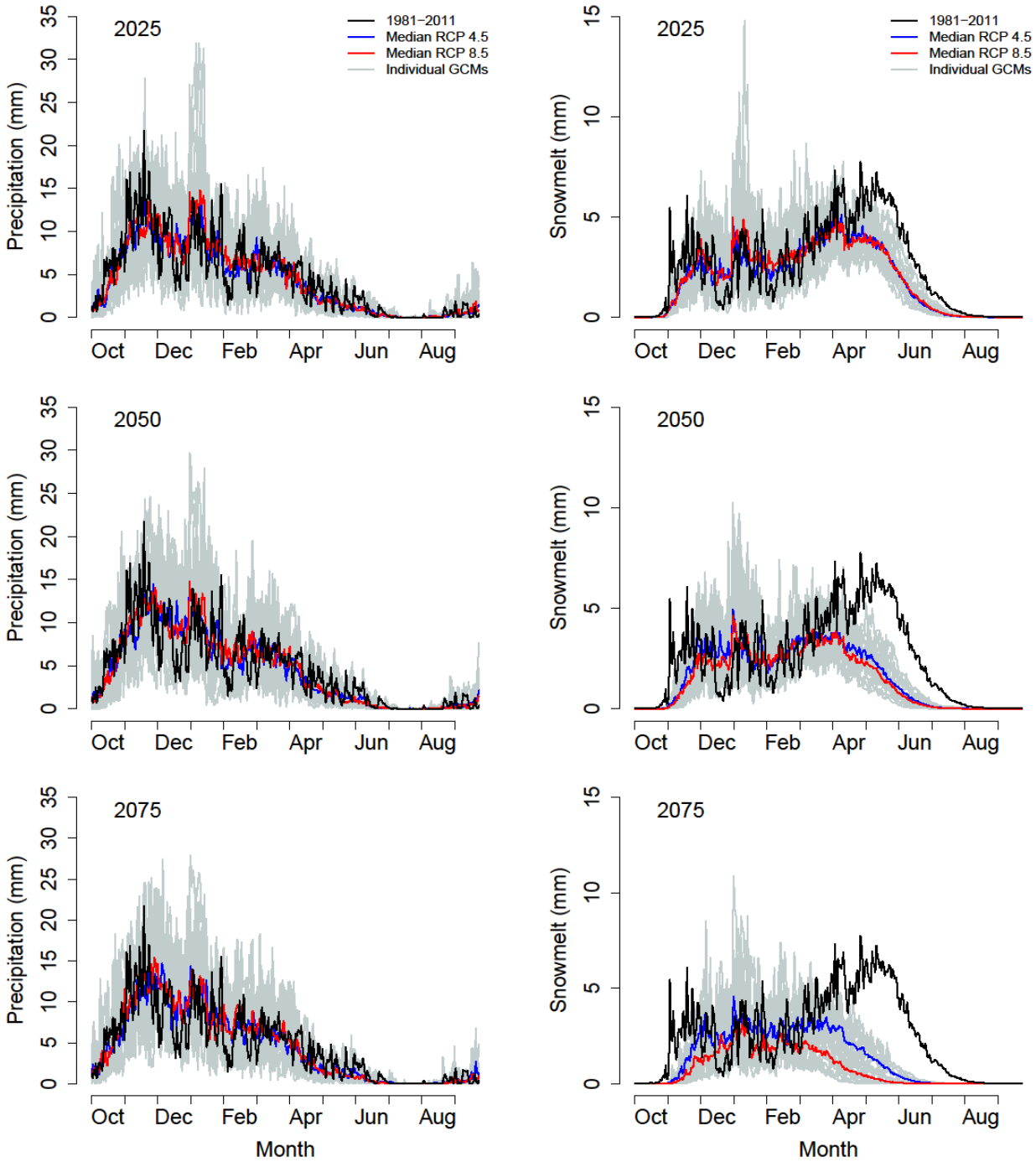

Figure 12. Monthly median sum of precipitation and snowmelt in the North Fork Stillaguamish basin over three 30-year climate normals centered on the years 2025, 2050, and 2075. Median hindcast values (30-year climate normal centered on the year 1996) are represented by the black line, the median RCP 4.5 values as the blue line, the median RCP 8.5 value as the red line, and individual GCMs by the grey lines.

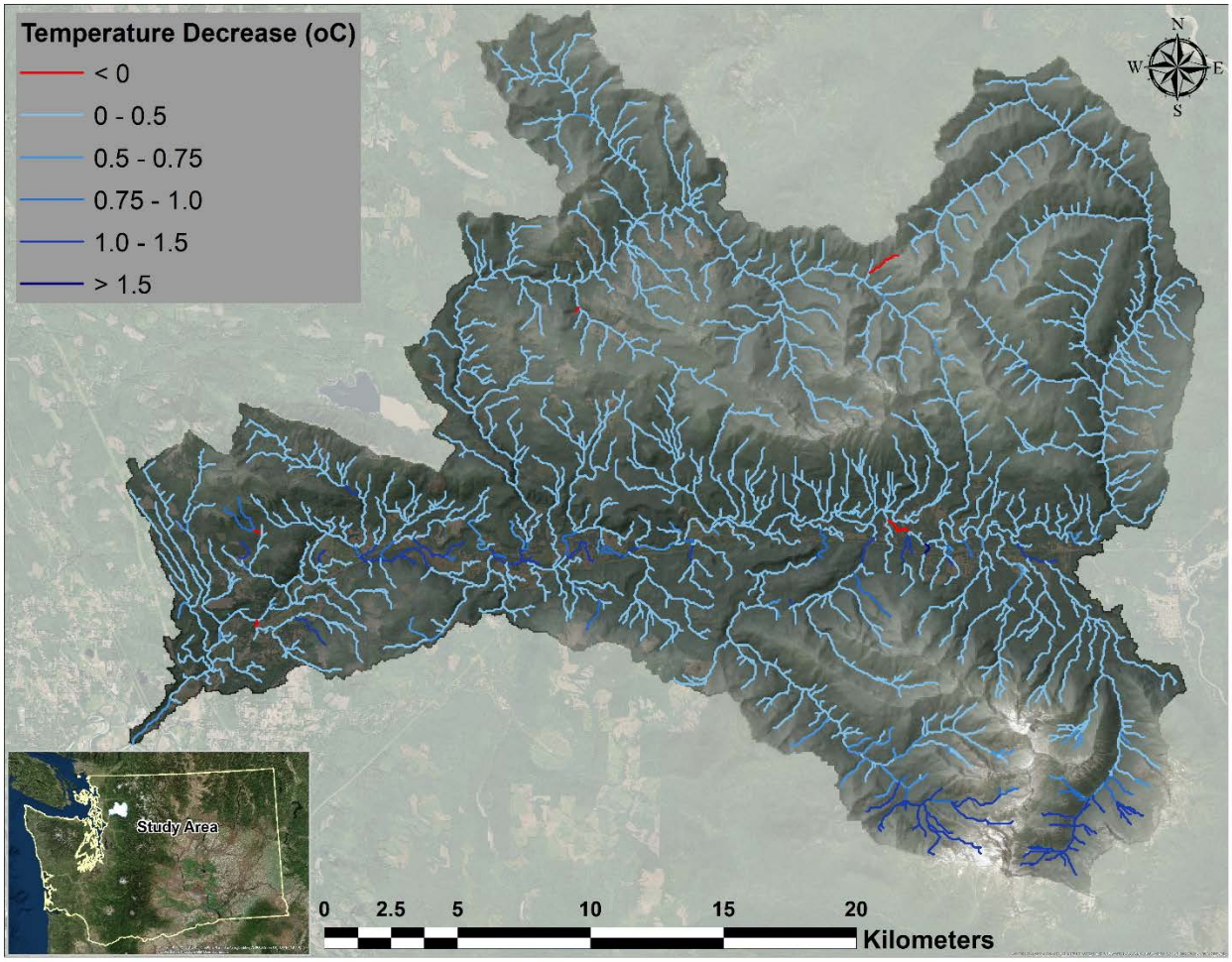

Figure 13. Average August stream temperature decrease at every stream segment in the North Fork Stillaguamish River between the CSIRO-Mk3-6-0 GCM under RCP 8.5 at the 2075 climate normal under present day riparian and land cover conditions, and the CSIRO-Mk3-6-0 GCM under RCP 8.5 at the 2075 climate normal under historic (1883) land cover and riparian conditions.

9.0 Appendix A

Riparian classification

By Kyra Freeman, June 2018

Part 1- Lidar set up

1. Download custom dataset using the polygon tool from the DNR LiDAR portal (http://lidarportal.dnr.wa.gov/). Create a polygon around your study area. Check just the DSM and DTM features to download.

E.g., LiDAR data in the North Fork Stillaguamish Basin

Dataset	Year	Resolution (feet)	Mosaic Operator
Darrington	2003	6	15
Glacier Peak	2010	3	8
Glacier Peak	2015	3	2
North Puget	2017	3	1
North Puget	2006	3	9
Puget Lowlands	2005	6	13
Snohoco Hazel	2006	3	11
Snohoco Oso- a	2014	3	4
Snohoco Oso- b	2014	3	5
Snohoco Oso- c	2014	3	6
Snohoco Sauk River	2005	6	14
Snohoco West	2006	3	10
Snohomish	2005	3	12
Stillaguamish	2014	3	3
Tualip 2013	2013	3	7

2. Mosaic them all together to a 6ft resolution: Data Management > Raster > Raster Dataset > Mosaic to new Raster

> Input Rasters: DSM datasets entered following the order of mosaic operator above. This was based on age of data collection, with the most recent datasets assumed to be the highest quality
> Output Location: E:\\WWU\ThesisGIS.gdb

Raster Dataset Name with Extension: DSM_6ft.tif
Pixel Type: 32_Bit_Float
Cell Size: 6 (should be the size of the largest dataset you are mosaicking)
Number of Bands: 1
Mosaic Operator: First (If you entered the datasets youngest first, enter Last if you started with the older datasets)
Mosaic Colormap: *leave blank*

*Note: The above operation will take a long time to process.

3. Repeat the above step with the DTM data in the same order.

Input Rasters: DTM datasets entered following the order of mosaic operator above.
Output Location: E:\\WWU\ThesisGIS.gdb
Raster Dataset Name with Extension: DTM_6ft.tif
Pixel Type: 32_Bit_Float
Cell Size: 6
Number of Bands: 1
Mosaic Operator: First (If you entered the datasets youngest first)
Mosaic Colormap: *leave blank*

4. Once you have both datasets, clip them to your basin.

WARNING! Do not do this with a raster layer of your basin. Use a polygon, otherwise the 6 ft resolution you had will be overwritten with the 50m resolution of your basin. In addition, it is important to do the same operations to both the DTM and DSM datasets, otherwise you will not be able to subtract them. The rows and columns of the DTM and DSM must match in order to determine tree height.

Spatial Analysis > Extraction > Extract by mask
Input: NF_DSM_6ft
Input mask: NF_mask (polygon file)
Output: NF_DSM_6ft

5. Repeat with DTM

Spatial Analysis > Extraction > Extract by mask
Input: NF_DTM_6ft
Input mask: NF_mask (polygon file)
Output: NF_DTM_6ft

6. Subtract the two datasets. Subtract the digital terrain model (DTM) from the digital surface model (DSM)

Spatial Analysis > Map Algebra > Raster Calculator
Expression: “NF_DSM_6ft” – “NF_DTM_6ft”
Output: NF_treeheight

7. Take a look at outliers. What is the range of your new “treeheight” layer? Ideally it will be 0 to ~300ft. Outliers are possible because of power lines, birds, etc. Double click on the layer, go to symbology, and change the stretched values to have 2 breaks. Manually change so that values below 0 are a separate color than 0-300, and >300 is a third color. Check how common outliers are. Are they concentrated to one area? If so, consider redoing the above steps without that section of the data, as long as there is older data that is also in that region. See file “LiDAR_DNR_correspondence.pdf” for more information about outliers from contacts at the DNR. If the outliers are few and have little chance of affecting your data, you can reclassify your treeheight file. Determine the average of the file by double clicking the layer, go to source, scroll down and record the mean.

Spatial Analysis > Reclass > Reclassify
Input: NF_treeheight
Old Value: -(lowest value) – 0 New Value: 0
Old Value: 300 (highest value) New Value: (basin average)
(Leave other values the same)
Output: NF_treeheight_r

Part 2- Create stream riparian buffer

Determine buffer width that you will use. You can experiment with several using the following steps and determine how the average tree height within each buffer changes. In ArcGIS, open the stream network that was developed from the soil depth file generation.

Geoprocessing > Buffer
Input Features: streamfile
Output Features: NF_buffer10m.shp
Distance: 10 Meters
Side Type: FULL
End Type: ROUND
Method: PLANAR
Dissolve Type: NONE

This will generate a file that has the same number of elements as stream segments. Each element will be a buffer of an individual stream segment.

Part 3- Use Model Builder Tool to extract tree height from each stream segment buffer area

1. Create a folder to direct individual stream segment rasters to. E.g., .../WWU/RBM/Riparian/seg_treeheight. This folder should be totally empty and only used for directing output from the next few steps.
2. Open ArcCatolog and navigate to tree_height.tbx Toolbox (supplied by Bob Mitchell). Right click on the Extract_stream_treeheight tool and click Edit.
3. Double click on the first element in the model builder. Navigate to your buffer, NF_buffer10m.shp as input.
4. Double click on the other element used as input, connecting to the Extract by Mask box. Navigate to your basin-wide LiDAR data file, NF_treeheight
5. Double click on the last element output called "Extr_%Value%". Do not change the name of the output but change the folder it goes to the folder you created in Step 1. E.g., .../WWU/RBM/Riparian/seg_treeheight/Extr_%Value%
6. Click on Model drop down menu. Click on Validate Model. If all the elements become colored, the model is ready to run. If not, go back and click through each one and ensure it is linked to the right field or folder.
7. Model > Run Entire Model. This may take hours, depending on how many stream segments there are.

Part 4- Use Python Script to determine mean value of each segments tree height raster

1. Navigate to "treeheight_mean.py" Python script. Right click > Edit with IDLE
2. Under Set environments, change the file path to the folder that you created in Part 3
3. Change the file path under the Local Variables section. Keep the treeheight.txt file name, and just change the location where you would like it saved.
4. Under the While True: loop, change the value in the except section to your basin-wide tree height average (in meters). This is to prevent the script from crashing if it encounters any problems in calculating the raster mean and will instead use the basin-wide average. This only happened in 3 instances in my script and may not be needed depending on if your LiDAR data has holes that encompass whole stream segments or not.

*Note, this script assumes that the LiDAR data is in feet and will convert results to meters.

5. File >Save, Run > Run Module

This may take several hours. When the script is done, you will have a file, treeheight.txt with two columns. First column is stream segment number, second column is the average tree height in a 10m area around that segment. Use this second column to copy and paste into the rveg.basline file that is read into RBM.